

Privacy–Utility–Bias Trade-offs for Privacy-Preserving Recommender Systems

SHIVA PARSARAD, University of Basel, Switzerland

ISABEL WAGNER, University of Basel, Switzerland

Recommender Systems (RSs) output ranked lists of items, such as movies or restaurants, that users may find interesting, based on the user’s past ratings and ratings from other users. RSs increasingly incorporate Differential Privacy (DP) to protect user data, raising questions about how privacy mechanisms affect both recommendation accuracy and fairness. We conduct a comprehensive, cross-model evaluation of two DP mechanisms, Differentially Private Stochastic Gradient Descent (DPSGD) and Local Differential Privacy (LDP), applied to four recommender systems (Neural Collaborative Filtering (NCF), Bayesian Personalized Ranking (BPR), Singular Value Decomposition (SVD), Variational Autoencoder (VAE)) on the MovieLens-1M and Yelp datasets. We find that stronger privacy consistently reduces utility, but not uniformly. NCF under DPSGD shows the smallest accuracy loss (under 10% at $\epsilon \approx 1$), whereas SVD and BPR experience larger drops, especially for users with niche preferences. VAE is the most sensitive to privacy, with sharp declines for sparsely represented groups.

The impact on bias metrics is similarly heterogeneous. DPSGD generally reduces the gap between recommendations of popular and less popular items, whereas LDP preserves existing patterns more closely. These results highlight that no single DP mechanism is uniformly superior; instead, each provides trade-offs under different privacy regimes and data conditions.

Additional Key Words and Phrases: Recommender systems, Bias, Differential privacy

ACM Reference Format:

Shiva Parsarad and Isabel Wagner. 2025. Privacy–Utility–Bias Trade-offs for Privacy-Preserving Recommender Systems. 1, 1 (December 2025), 34 pages. <https://doi.org/10.1145/nnnnnnn.nnnnnnn>

1 Introduction

Recommender Systems (RSs) are mechanisms for filtering information and presenting personalized ranked lists of items to users. RSs are widely used for a variety of applications, e.g., books, news, or movies, thanks to their ability to filter and rank vast amounts of information available online.

However, past user data can reveal sensitive personal information [10, 23, 59, 61, 63, 72]. For example, our preferred movie genres can expose our personality traits [31] or be used for advertising purposes. To address these privacy concerns, privacy-preserving recommender systems have been proposed, often based on a form of Differential Privacy (DP). DPSGD, for example, applies DP during the training process of a machine learning model, thereby guaranteeing privacy for the trained model [1], whereas LDP applies DP to each user’s data before training the recommender model [52]. While these techniques provide provable privacy guarantees, they may degrade recommendation quality, and increasingly, it is recognized that privacy mechanisms can also influence bias and fairness in RSs [19, 52]. Recommender Systems (RSs) suffer from well-known biases, for example, RSs can influence which information is readily available to

Authors’ Contact Information: Shiva Parsarad, University of Basel, Basel, Switzerland, shiva.parsarad@unibas.ch; Isabel Wagner, University of Basel, Basel, Switzerland, isabel.wagner@unibas.ch.

Permission to make digital or hard copies of all or part of this work for personal or classroom use is granted without fee provided that copies are not made or distributed for profit or commercial advantage and that copies bear this notice and the full citation on the first page. Copyrights for components of this work owned by others than the author(s) must be honored. Abstracting with credit is permitted. To copy otherwise, or republish, to post on servers or to redistribute to lists, requires prior specific permission and/or a fee. Request permissions from permissions@acm.org.

© 2025 Copyright held by the owner/author(s). Publication rights licensed to ACM.

Manuscript submitted to ACM

Manuscript submitted to ACM

1

users because users rarely visit search results beyond the first page [32], and they can skew recommended item lists towards popular items, thereby reducing the relevance of recommended items to users with niche tastes [22].

Although the impact of RS on privacy and bias is known, research on these issues remains largely separate, i.e., the important question of how privacy mechanisms influence bias in RSs remains understudied. Most prior work studies privacy and fairness separately or evaluates only specific models and specific kinds of bias [52]. A few works consider fairness across user or item groups [18], but the broader question of how different DP mechanisms influence utility and bias across different user groups, item types, and model architectures is still underexplored. This is an important gap because different RS models have different sensitivities to noise: deep neural RSs may absorb noise through high-capacity representations, matrix-factorization methods rely on low-dimensional latent factors that are more fragile under perturbation, and generative models such as VAEs can collapse under high sparsity. Understanding these differences is essential for deploying privacy-preserving systems that are both accurate and debiased.

To close this gap in knowledge, we study the following research questions: How do DPSGD and LDP affect ranking utility? How do privacy mechanisms influence bias metrics such as miscalibration, popularity lift, novelty, coverage, and producer fairness? How are niche, diverse, and blockbuster users affected differently? Under what conditions can private RSs maintain acceptable accuracy without increasing bias?

In this work, we systematically examine the trade-offs between privacy, utility, and bias across four representative families of RS models including SVD, BPR, NCF, and VAE, using two real-world datasets (MovieLens-1M and Yelp) and two DP mechanisms (DPSGD and LDP). Our study spans a wide range of privacy budgets (ϵ), multiple user and item subgroups, and five complementary bias metrics. Our main contributions are as follows:

- **Comprehensive evaluation of DP mechanisms across model families.** We implement and analyze DPSGD and LDP across four representative recommender-system architectures: SVD, BPR, NCF, and VAE.
- **Analysis across multiple privacy levels and datasets.** We evaluate the impact of both DP mechanisms over a wide range of privacy budgets (ϵ), using two widely adopted benchmark datasets: MovieLens 1M and Yelp.
- **Utility and bias trade-off evaluation.** We measure ranking quality (NDCG) and assess multiple bias dimensions, including miscalibration, popularity lift, novelty, item coverage, and deviation from producer fairness.
- **Fine-grained examination of group fairness¹ across user and item subgroups.** We analyze impacts across different user profiles (niche, blockbuster, and diverse) and item categories (popular vs. unpopular), revealing heterogeneous fairness impacts across sub-populations.
- **Identification of privacy–fairness “sweet spots”.** We uncover privacy regimes, especially moderate ϵ that offer strong utility with only mild changes in bias, while also highlighting conditions where no such sweet spots exist (e.g., VAE on sparse data).

Our findings show that the impact of Differential Privacy (DP) on utility and bias is highly dependent on the choice of DP mechanism, the underlying model architecture, and dataset characteristics. NCF trained with DPSGD maintains high utility (within 10% of non-private performance) even under strong privacy ($\epsilon \approx 1$), forming a clear sweet spot where utility remains high and most bias metrics remain within their acceptable ranges (e.g., no extreme positive or negative Popularity Lift (PL)). In contrast, SVD, and BPR show moderate sensitivity to privacy mechanisms, and VAE collapses under increased sparsity, offering no meaningful sweet spots. Bias outcomes vary similarly: miscalibration is mostly stable except for NCF/Yelp; Deviation from Producer Fairness (DPF) ranges widely (≈ -0.8 to $+1.0$), with DPSGD reducing head–tail distinctions at low ϵ and LDP preserving baseline biases.

¹Please note that in this paper, we interpret fairness as reduced or controlled bias, and we measure it using bias-oriented metrics.

Overall, our findings show that no single DP mechanism is universally superior. Instead, the best privacy–utility–bias trade-off depends on the model architecture, dataset sparsity, and user or item subgroup. These insights help guide the deployment of privacy-preserving recommender systems that balance privacy, accuracy, and fairness in practice.

2 Background and Related Work

2.1 Recommender systems

The three main types of RSs involve collaborative filtering, content-based filtering, and hybrid approaches. The most common technique used for recommendations is collaborative filtering. In this paper, we investigate several methods for recommendation systems, including ranking-based Bayesian Personalized Ranking (BPR), matrix factorization methods such as Singular Value Decomposition (SVD), hybrid models like Neural Collaborative Filtering (NCF), and Variational Autoencoders (VAEs) [44]. BPR and SVD are both collaborative filtering methods based on matrix factorization. NCF is a hybrid model that combines neural network architectures with collaborative filtering principles. Variational Autoencoders (VAEs) are also used for collaborative filtering with implicit feedback.

BPR is an optimization criterion based on the maximum posterior estimator which enables us to train models that are optimized for ranking instead of the item prediction task [64]. The training data, D_s consists of tuples (u, i, j) , meaning that user u prefers the positive item i over the negative item j . To maximize the posterior probability, BPR uses stochastic gradient descent. BPR can support learning different model classes, including k-nearest-neighbor and matrix factorization, used for recommender systems

SVD decomposes a user-item interaction matrix R into three matrices: U containing user-specific latent factors, Σ containing singular values that scale the latent factors, and V containing item-specific latent factors. By truncating Σ and the corresponding columns of U and V to the top k components, SVD reduces the dimensionality of R , capturing the most significant underlying structures while reducing computational complexity. The resulting low-rank approximation $\hat{R} = U_k \Sigma_k V_k^T$ estimates the ratings matrix, predicting unknown ratings and revealing patterns in user-item interactions [49].

RSs based on deep learning, such as NCF [34], can overcome limitations of traditional models and achieve better performance [77]. Specifically, a NCF model that combines a Multilayer Perceptron and Matrix Factorization (MF) to predict user interests showed significant improvements in performance compared to conventional approaches [34]. In this paper, we use the same architecture for the deep recommender system we investigated.

VAEs generalize traditional latent-factor models by introducing non-linear, probabilistic latent variables through neural networks. For each user u , a latent representation \mathbf{z}_u is sampled from a prior distribution $\mathbf{z}_u \sim \mathcal{N}(0, I)$. The user-item interactions \mathbf{x}_u are then generated by using a multinomial likelihood $\mathbf{x}_u \sim \text{Multinomial}(N_u, \text{softmax}(f_\theta(\mathbf{z}_u)))$.

The model is trained by maximizing the Evidence Lower Bound (ELBO), which balances reconstructing the observed data and regularizing the latent space:

$$\mathcal{L}(\mathbf{x}_u; \theta, \phi) = \mathbb{E}_{q_\phi(\mathbf{z}_u | \mathbf{x}_u)} [\log p_\theta(\mathbf{x}_u | \mathbf{z}_u)] - \text{KL}(q_\phi(\mathbf{z}_u | \mathbf{x}_u) \parallel p(\mathbf{z}_u))$$

Balanced approach enables VAEs to capture complex patterns in the data, significantly improving recommendation performance on large datasets [44].

2.2 Privacy Challenges and Solutions in Recommender Systems

Recommending items based on a user’s preferences or past interactions leads to privacy issues, including: (i) personal data breaches, (ii) leaking of information that can enable user tracking, and (iii) the disclosure of user preferences via recommendations [26, 35]. For example, an attacker can reveal sensitive information, such as the age of users, from a variational autoencoder recommender (VAE) system [27]. To this end, once the training of VAE is complete, an attacker network is introduced to the model, which aims to predict sensitive attribute age from the latent vector. Even approaches that are designed to enhance transparency in RSs can compromise user privacy. For instance, in the domain of social media, when a system seeks to provide explanations for its recommendations by citing the interests of friends, it risks violating the privacy of those individuals [29].

Approaches to protect user privacy include methods based on differential privacy, methods focusing on specific parts of the data, and methods based on recommendation unlearning. Generally, DP proposed to minimize the likelihood of inferring the presence or absence of any specific record in the input. DP provides a theoretical privacy guarantee, the strength of which is governed by the proper privacy budget ϵ , where smaller ϵ indicates higher privacy protection. (ϵ, δ) -DP, called *approximate differential privacy*, is a more relaxed version of DP, where δ bounds the probability that the privacy guarantee fails, and such failures happen with at most probability δ . A randomized mechanism M is considered (ϵ, δ) -DP if the probability of a privacy leakage is no more than δ :

$$\Pr [M(D) \in S] \leq e^\epsilon \cdot \Pr [M(D') \in S] + \delta \quad (1)$$

There are several strategies for integrating DP into RSs, each targeting different aspects of the process. One approach focuses on applying DP to input data. For instance, a DP-based method employs k-means clustering and utilizes an exponential mechanism to implement differentially private user-based collaborative filtering [14]. Similarly, randomized response is used as a local differential privacy technique to ensure input data privacy [52]. Another category incorporates noise directly into the objective function during training to achieve differential privacy. For example, an auto-encoder-based recommender system that adds noise to the objective function [24]. In addition to these methods, some approaches utilize embeddings to apply DP during the transformation of raw data into feature representations. Embedding-Aware Noise Addition (EANA) [55] selectively adds noise to parameters with non-zero gradients. EANA improves the efficiency of training embedding-based neural networks with DP, although it provides privacy guarantees only if the adversary has access solely to the final trained model.

In addition to the aforementioned approaches, another method incorporates DP mechanisms into the gradients during model training. Differentially private stochastic gradient descent (DPSGD), introduced for deep learning [1], is a generic technique that ensures differential privacy for any training process performed with SGD by using the Gaussian mechanism to add noise to the clipped gradients [25]. A variation of DPSGD uses Stochastic Gradient Langevin Dynamics (SGLD) to build a differentially private recommendation system based on matrix factorization [47]. However, SGLD is slower than SGD and complete models have the convergence problem [47].

One of the main challenges with DP is the privacy–utility trade-off, which arises from the noise introduced to ensure privacy. To address this issue, several innovative approaches have been proposed to improve privacy without necessarily applying noise. One such approach is recommendation unlearning, which is used when a recommender system needs to forget certain sensitive data and its complete lineage. “Influence function” is an example to achieve recommendation unlearning without model retraining [78]. While this method can reduce the risk, it cannot ensure that all sensitive information linked to a specific user is entirely eliminated.

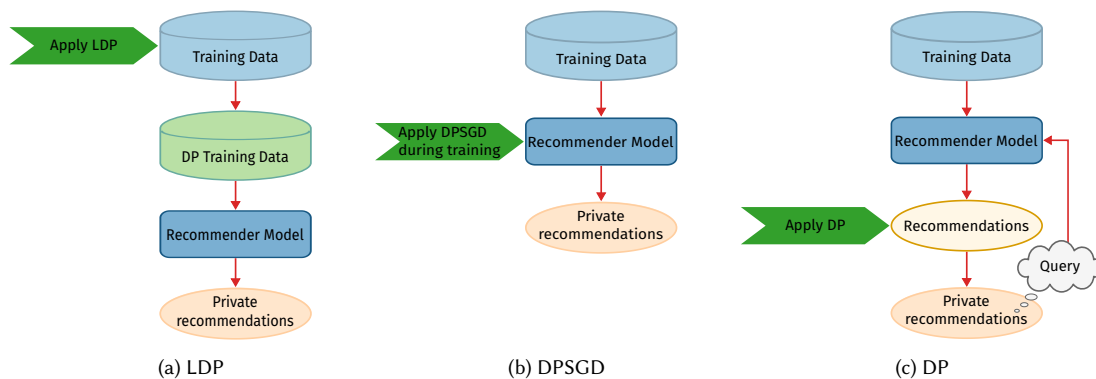


Fig. 1. Three approaches for creating differentially private recommender systems: applying LDP to training data, applying DPSGD during model training, and applying DP to generated recommendation lists.

Additionally, another approach focuses on limiting the amount of user interaction history. Therefore, rather than considering a user’s entire history, a few carefully selected interactions are sufficient to achieve high personalization quality and thus improve privacy [65]. However, reducing a user’s history—such as removing ratings for certain items—can increase the system’s vulnerability to data poisoning attacks [67]. Similarly, focusing on user interactions rather than content or messages is a means to improve privacy [69]. Recent research, however, indicates that various types of user-sensitive information—such as age, gender, occupation, and even political orientation—can be inferred from user-item interactions [74]. Additionally, Federated Learning, as one of the promising approaches, can still leak sensitive user information if DP mechanisms are not applied [11].

Considering the challenges and solutions discussed, there are findings [5] that DPSGD provides better privacy protection even at high values of epsilon, outperforming several newly proposed privacy-enhancing approaches. Therefore DPSGD could be regarded as the best-in-class defense for practical applications [5].

In general, as Figure 1 shows, there are three DP-based methods. One option is to introduce controlled noise to the training data before commencing the training process; a technique like randomized response, depicted in Figure 1a, is an example of this approach and is discussed in greater detail in Section 3.1.1. Another widely-used method involves adding controlled noise during the training phase, which is particularly common for deep models, as shown in Figure 1b. This approach is discussed in Section 3.1. The final option, illustrated in Figure 1c, entails training the model without any modifications and subsequently introducing noise to its outputs. However, this method has a significant drawback: the privacy loss compounds with each query made to the model, necessitating noise additions that are proportional to the number of queries. As a result, this can lead to outputs that are effectively unusable.

2.3 Bias in Recommender Systems

Recommender systems can amplify biases, including position bias, selection bias, popularity bias, and representation bias [13]. These biases can distort recommendation outcomes in various ways. For instance, they can lead to ranked lists that do not provide equal coverage to items throughout the whole popularity range [73], reinforce filter bubbles [54], and skew user engagement [3].

Bias in recommender systems can be categorized in multiple ways, including group vs individual fairness and single-sided vs. multi-sided bias [18]. Individual fairness refers to the principle that candidates with similar characteristics

should be treated similarly [18]. With group fairness, the goal is to achieve statistical parity between protected groups. To evaluate group fairness, the users or items are divided into non-overlapping groups based on some attributes. For example, users can be divided based on the types or categories of items they consume, and items can be divided based on their popularity.

Research on recommender systems often focuses on their value to consumers, which corresponds to single-sided fairness [18]. Multi-sided fairness considers fairness from the viewpoint of multiple stakeholders, such as consumers and item providers [18]. What may be a fair recommendation for users is, in some way, unfair to the item provider. Here, items are categorized according to their popularity, and users according to the popularity of items they consume.

In general, approaches for solving bias can be categorized into three main types: those that use de-biasing as a post-processing method, those that incorporate bias mitigation into their objective function, and those that aim to create de-biased representation vectors. For example, calibration is a post-processing approach that ensures that recommendation lists reflect the distribution of user preferences [68]. It achieves by pushing the model towards generating balanced recommendation lists [13]. Similarly, re-ranking techniques can optimize relevance scores while simultaneously reducing both item and consumer bias [62].

To address bias as part of the objective function, off-policy learning combined with an additional cost function can improve item exposure fairness [71]. To enforce fairness, the Exact-K-Fairness constraint ensures that the proportion of item exposure between head-tailed and long-tailed groups remains statistically indistinguishable. Some methods [43] focus on de-biased representation learning, for example, by making node representations fairer by alleviating the popularity bias in learning the representation of users and items, and tune neighbors' weights based on their popularity levels. Additionally, when only biased feedback is available, it is possible to focus on mitigating confounding bias through debiased representation learning [46].

Several metrics help quantify bias in recommender systems. For example, higher entropy values indicate better item fairness, while the Gini index measures inequality in the item distribution [17]. Additionally, the Herfindahl-Hirschman Index (HHI) assesses the concentration of recommendations among items [17], and head-tail ratio and the Gini index evaluate fairness [71]. The normalized Gini index assesses the inequality and the average percentage of long-tail items to evaluate the presence of popularity bias in recommendations [48]. Additionally, item coverage evaluates how well the recommended items span the entire range of products [48]. For considering both consumer and product fairness, a division categorizes items into two categories based on their popularity: short-head and long-tail items [62]. The deviation-from-parity exposure metric identifies whether short-head or long-tail items receive disproportionate exposure. Similarly, a grouping separates users based on their activity levels. The deviation-from-parity consumer fairness metric evaluates whether fairness holds across different user groups. The limitation of the proposed metrics are that they are only applicable when there are two user groups.

Popularity bias occurs when popular items receive increased visibility in recommendation lists, leading to a subsequent increase in their consumption rate. Popularity Lift is a metric to evaluate the degree of amplification of popularity bias in the user profile and the generated recommendation lists for different user groups [3]. In addition to the approaches discussed earlier, methods such as novelty, miscalibration, and coverage are also used to evaluate the bias state of recommendation lists, which will be explained in detail in Section 3.3.

2.4 The Privacy-Bias Trade-off in Recommender Systems

DP ensures that algorithms behave similarly on any pair of databases differ only in the data of a single individual [21]. This definition aligns with fairness, which requires outcomes of the model to remain similar for similar individuals

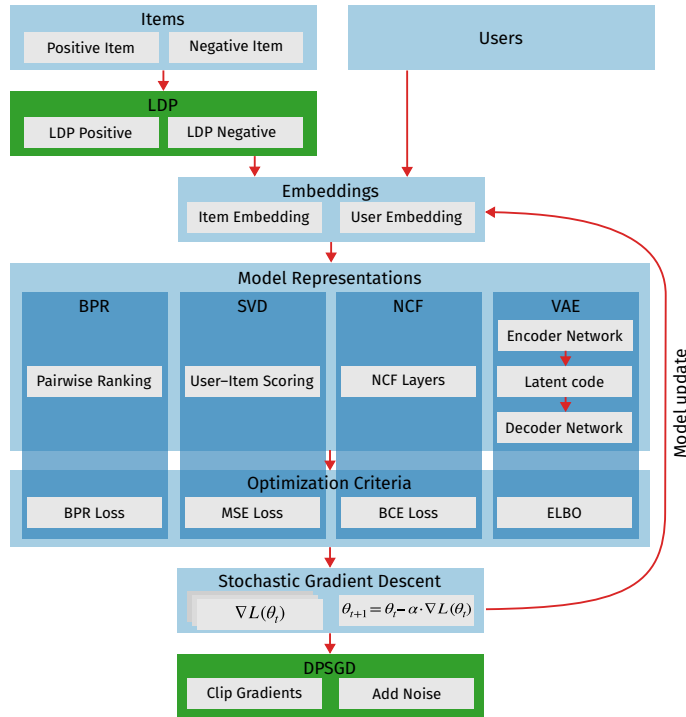


Fig. 2. General Process of Applying LDP and DPSGD to Models

[76]. Therefore, privacy can promote fairness or decrease bias, and fairness or debiasing, in turn, can enhance privacy. Also, breaking the user’s privacy can be disparately successful against minority groups in some cases [50]. A violation of privacy can result in unfairness or bias because of an adversary’s capability to infer sensitive information about individuals [60]. Some methods proposed to reduce bias also enhance privacy [27].

However, in general, there has been limited research on how privacy-enhancing methods impact various bias metrics [51]. In machine learning, privacy protections can negatively impact fairness, for example through a disproportionate reduction in model accuracy for underrepresented subgroups [8]. A recent study examined the correlation between differential privacy and bias in recommender systems [52]. That work applied DP to user data rather than the training process and focused exclusively on deep recommender architectures, with a particular emphasis on how DP influences popularity bias. In contrast, in this paper, we examine how DPSGD affects utility and bias across four different classes of recommender systems. Since DP-SGD enforces privacy through modifications to the training procedure, we additionally compare its effects with LDP mechanism [52].

3 Methods

Our main goal is to study the trade-offs between privacy, performance, and bias in recommender systems. We perform this study on four different types of recommender systems, each in a private and non-private version (Section 3.1), applied to two datasets (Section 3.2), by using a range of metrics (Section 3.3) and experimental settings (Section 3.4). Table 2 summarizes the notation used in this paper.

3.1 Privacy-preserving recommender systems

To enhance privacy in recommender systems, two primary approaches leverage differential privacy: LDP and DPSGD. LDP protects user data at collection by adding randomness, while DPSGD ensures privacy during model training by clipping gradients and injecting noise. Figure 2 shows the integration of LDP and DPSGD at different stages of the recommendation process. User and item embedding updates are treated as optimization problems, which enables the application of DPSGD. Figure 2 differentiates where each privacy method is applied. LDP is applied before the embedding stage, specifically on the item interaction data. This means that items are perturbed locally on the client side before they are embedded, resulting in noisy or DP-based embedding representation. In contrast, DPSGD is applied during the training process.

Each model block in the Figure 2 shows its unique approach to generating the recommendation list. For example, NCF uses a stack of neural network layers (NCF layers) to learn interactions between user and item embeddings. Similarly, BPR and SVD rely on pairwise ranking and matrix factorization mechanisms, respectively. For SVD, we represent users and items using latent embedding vectors and train these embeddings with SGD to facilitate the application of DPSGD. For BPR, the process of updating user and item embeddings is expressed as a stochastic optimization problem similar to SGD, which iteratively adjusts user and item embeddings. In each training step, given a positive user–item interaction, the model updates the embeddings to improve the ranking of positive interactions over negative ones. VAE adopts an encoder-decoder structure with latent variables for probabilistic modeling. Each model is trained by minimizing its own loss function: Mean Squared Error (MSE) Loss for SVD, BPR Loss for BPR, Binary Cross Entropy (BCE) Loss for NCF, and ELBO for VAE. These loss functions serve as the optimization criteria guiding model updates. When DPSGD is applied, it modifies this optimization process by introducing noise and clipping gradients, making privacy a built-in part of training rather than a pre-processing or post-processing step.

3.1.1 Recommender Systems with Local Differential Privacy. One way to apply DP to recommender systems is randomized response [52]. Randomize response flips a fair coin to decide whether to report the true response or the opposite [21]. Inspired by the 1-Bit mechanism for mean estimation [20], a Local-DP mechanism can be used to randomize the selection of positive feedback in recommender systems [52]. Local-DP mechanism protects user privacy in systems that rely on binary implicit feedback by introducing randomness into the feedback selection process. Two types of feedback are considered:

- **Positive feedback** (D^+): Interactions where a user expresses a preference for an item (e.g., a click, like, or purchase).
- **Negative feedback** (D^-): Instances where the user does not interact with an item or provides no feedback.

In scenarios with explicit ratings, items can be classified into positive and negative feedback categories using a threshold on the ratings. Items with ratings exceeding the threshold are categorized as D^+ , while all other items are treated as D^- . The probability P_{D^+} of including a positive feedback item in the differentially private positive dataset is given by:

$$P_{D^+} = \frac{1}{e^\epsilon + 1} + \frac{e^\epsilon - 1}{e^\epsilon + 1} \quad (2)$$

The first term introduces randomness, while the second term adjusts this randomness based on the privacy budget, where higher values of ϵ lead to a higher chance of including positive feedback, resulting in a dataset that is less private but more accurate.

Similarly, the probability that a negative or missing feedback item will be included in the new DP positive dataset is calculated as follows:

$$P_{D^-} = \frac{1}{e^\epsilon + 1} \quad (3)$$

This probability is lower than the probability for positive feedback, ensuring that negative or missing feedback data is added with lower likelihood. In this approach, only positive feedback is perturbed, as it represents explicit user preferences (e.g., what a user explicitly likes or purchases) that are more likely to reveal personal information. Because negative feedback is implicit (e.g., lack of interaction) and less informative, it may not require the same level of perturbation to achieve privacy guarantees.

3.1.2 Recommender Systems with Differential Private Stochastic Gradient Descent. DPSGD is a technique to ensure privacy protection during the training process of deep learning models [1]. And is therefore a natural fit for deep recommender systems. Consider a user u with k positive interactions represented as $u_p = x_1, x_2, \dots, x_k$. Suppose we have a recommender system designed to optimize a loss function L , such as MSE, and BCE. The primary goal of such systems is to predict items that a user is likely to be interested in based on their past interactions u_p .

Using Stochastic Gradient Descent (SGD) on a recommender system involves iteratively minimizing the loss function L . DPSGD introduces a privacy-preserving approach to this process [1]. At each iteration, a batch of user interactions x_i is sampled from the training dataset. This batch includes a subset of positive interactions, and for some models, both positive and negative interactions u_p from each user. The size of the batch is typically fixed and is determined based on the system’s capacity and the desired trade-off between computation and privacy. To control the influence that any single data point has on the model, each gradient $\nabla_{\theta}L(\theta, x_i)$ or g is clipped by using the ℓ_2 -norm. Specifically, the gradient is rescaled to ensure that its ℓ_2 -norm does not exceed a predefined threshold C . The clipping norm C determines the maximum allowed ℓ_2 -norm of the gradients.

$$\bar{g}(x_i) = \nabla_{\theta}L(\theta, x_i) / \max\left(1, \frac{\|\nabla_{\theta}L(\theta, x_i)\|_2}{C}\right) \quad (4)$$

This step prevents any individual example from disproportionately affecting the model. Once the gradients for each data point in the batch are computed and clipped, the average of the gradients is calculated:

$$\bar{g} = \frac{1}{B} \sum_{i=1}^B \bar{g}(x_i) \quad (5)$$

where B is the size of the batch. To ensure differential privacy, noise is added to the aggregated gradient. The noise is drawn from a Gaussian distribution with mean zero and a variance scaled by $\sigma^2 C^2$. The amount of noise is controlled by the noise multiplier σ , which governs the trade-off between privacy and utility.

$$\tilde{g} = \bar{g} + \mathcal{N}(0, \sigma^2 C^2 I) \quad (6)$$

Finally, the model parameters θ are updated in the opposite direction of the noisy gradient. The update is performed by subtracting the noisy gradient scaled by the learning rate η :

$$\theta = \theta - \eta \cdot \tilde{g} \quad (7)$$

The algorithm repeats the process for a set number of iterations or until convergence, where convergence is typically determined by the stability of the loss function or parameter updates. The privacy cost of the entire training process is tracked by a privacy accountant, such as the moments accountant [1], Rényi Differential Privacy (RDP) accountant, or

	Yelp	MovieLens 1M
Total items	7,156	3,258
Total users	9,872	6,038
# of interactions	175,767	835,614
% of interactions	0.24%	4.22%
# of item categories	1030	19
Min categories per item	1	1
Max categories per item	25	7
Mean categories per item	4.36	2.11

Table 1. Comparison of item statistics between Yelp and MovieLens 1M datasets.

Privacy Random Variables (PRV) accountant [30] that tracks the privacy loss more accurately than RDP or the classical moments accountant. These techniques ensures an overall privacy bound of $O(q\epsilon T, \delta)$ -differential privacy, where T represents the number of gradient descent steps, and q the batch sampling probability.

3.2 Datasets

The MovieLens 1M dataset has a total of 1,000,209 ratings provided by 6,040 individuals for 3,706 movies [33]. Movies are categorized in 20 genres. The Open Yelp dataset contains 6,990,280 reviews for 150,346 businesses, categorized in 1030 business types. Both Open Yelp and MovieLens 1M use ratings between 1 (lowest) and 5 (highest).

We clean both datasets in line with prior work. In particular, we exclude all ratings below three, all items with less than five ratings, and all users who have rated less than five items [15, 34]. In addition, following the common practice of restricting the Yelp dataset to specific regions [42], we limit our analysis to businesses in Arizona (AZ area). After preprocessing, we have 835,614 ratings in the 1M dataset (3,258 movies and 6,038 users) and 175,767 ratings in the Yelp dataset (7,156 businesses and 9,872 users). Table 1 shows the statistics of these two datasets after all pre-preprocessing steps. Compared to 1M, the Yelp dataset is significantly more sparse. Despite having more users and items, Yelp contains fewer overall interactions, which results in an interaction density of just 0.24%, in contrast to 4.22% in 1M. Moreover, Yelp includes a much larger and more diverse set of item categories (1,030 vs. 19), with a higher average number of categories per item (4.36 vs. 2.11).

We employ an 80/10/10 data split for training, testing, and validation, splitting on a *per-user* basis. This ensures that each user in the test/validation sets has a history in the training set.

3.2.1 User types. We divide users into three categories – niche, blockbuster, and diverse – based on the popularity of items they have rated [3]. Items are called *popular* if they are in the top 20% of items sorted by popularity. Niche users prefer unpopular items, i.e., less than 50% of items in their profiles are popular, whereas blockbuster users have more than 85% of popular items in their profiles. All other users are called diverse. The distribution of user types (see Figures 3a and 3b) shows that the Yelp dataset contains significantly more niche users, and fewer blockbuster users, than 1M.

3.2.2 Item popularity. In addition to examining different user categories, we also evaluate the behavior of recommender systems on two categories of items: the short head and the long tail, which are defined based on item popularity [2, 62]. Each item belongs exclusively to either I_1 or I_2 , so $I_1 \cap I_2 = \emptyset$. The top 20% of items are classified as I_1 , while the remaining 80% are considered as long-tail or unpopular items (I_2). By categorizing the items into short head and long tail, we can assess the performance of recommender systems in terms of how they handle the recommendation of popular

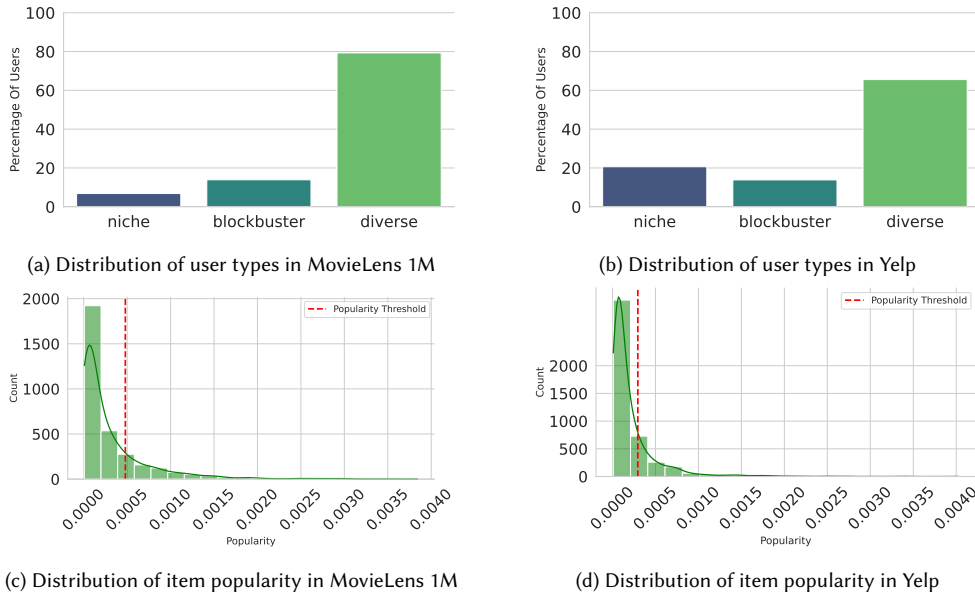


Fig. 3. Distribution of user types and item popularity in Yelp and MovieLens datasets

versus unpopular items. Figures 3c and 3d show the popularity distribution of items in each dataset. The majority of items are to the left of the threshold line, classified as unpopular items I_2 , while those to the right are considered as I_1 .

3.3 Metrics

We use a set of metrics to comprehensively evaluate utility, bias, and privacy of RSs. Our selection ensures that the evaluation covers different aspects of how an RS performs [75] and includes the most common metrics in RS evaluation [9].

3.3.1 Utility Metrics. We use Recall, Normalized Discounted Cumulative Gain (NDCG@10), and Mean Reciprocal Rank (MRR) to evaluate the ranking quality, or utility, of recommender algorithms. However, due to the similarity in trends across these metrics, we only report results for NDCG.

Normalized Discounted Cumulative Gain. NDCG measures how closely the predicted ranking of items aligns with the ideal ranking, taking into account the relevance of each item [39]. The DCG for the first p items is given by:

$$DCG_p = \sum_{i=1}^p \frac{2^{\text{rel}_i} - 1}{\log_2(i + 1)}$$

where rel_i is the relevance score of the item at position i , and p is the number of ranked items. The Normalized Discounted Cumulative Gain is obtained by normalizing DCG_p with the ideal DCG ($iDCG_p$). A perfect ranking results in $nDCG = 1$, with any deviation leading to a score less than 1.

Table 2. Notation used throughout this paper

Symbol	Meaning
ϵ	Privacy Budget
δ	Probability of the privacy leakage
D^+ / D^-	Positive feedback/ Negative feedback
P_{D^+} / P_{D^-}	Probability of including a positive/negative feedback item in the new DP positive dataset
C	clipping norm
σ	Noise Multiplier
θ	Model weights
\bar{g}	Average of Gradient
B	Batch Size
$L(\theta, x_i)$	Loss function evaluated for input x_i and model parameters θ
I, I_1, I_2	Set of the items, Popular Items, Unpopular Items
$q(z u)$	Distribution of genres/business-styles z in the list of movies/businesses recommended to user u
$p(z u)$	Distribution of genres/business styles z in the set of movies/businesses H previously rated by user u
$nDCG_p$	Normalized Discounted Cumulative Gain
$C_{KL}(p, q)$	Miscalibration based on KL divergence
$GAP(G)$	Group Average Popularity
$PL(G)$	Popularity Lift
π_i	Popularity of item i
G	Users' group, such as niche or blockbuster
R	The recommended list
$Novelty(R)$	Novelty of R recommended items
$Coverage$	Percentage of total items I that are recommended
DPF	Deviation from Producer Fairness

3.3.2 *Bias Metrics.* To evaluate biases in recommender systems, we used five different bias metrics to assess different aspects of bias: group fairness (miscalibration), popularity bias, novelty, item coverage, and item fairness (deviation from producer fairness).

Miscalibration. Miscalibration measures to what extent the item category distribution in a user's history deviates from the distribution in the recommended list. Miscalibration occurs when this alignment is poor, indicating that the recommender fails to reflect the user's true distribution of interests. Miscalibration can be seen as a measure of group fairness, even if item categories do not explicitly represent protected attributes [18].

We use the Kullback-Leibler Divergence (KLD) to measure the miscalibration of recommended item lists [68]. In general, KLD is a measure for the distance between two distributions. Here, we consider the distribution of genres/business-styles in the list of recommended items and in the user's rating history. The distribution of genres/business-styles z in the list of movies/businesses recommended to user u is denoted as $q(z|u)$:

$$q(z | u) = \frac{\sum_{i \in R} w_{u(i)} p(z | i)}{\sum_{i \in R} w_{r(i)}} \quad (8)$$

Similarly, the distribution of genres/business styles z in the set of movies/businesses H previously rated by user u is denoted as $p(z|u)$:

$$p(z | u) = \frac{\sum_{i \in H} w_{u,i} p(z | i)}{\sum_{i \in H} w_{u,i}} \quad (9)$$

I is the set of recommended items, and $w_{u(i)}$ is the weight of item i based on its rank r_i in the recommendation list. And finally, the calibration metric C_{KL} based on KL divergence is calculated as follows:

$$C_{KL}(p, q) = KL(p||\tilde{q}) = \sum_g p(z|u) \log \frac{p(g|u)}{\tilde{q}(z|u)} \quad (10)$$

Where $w_{u,i}$ is the weight of movie i , e.g., how recently it was played by user u . If $q(g|u)$ and $p(g|u)$ are similar, C_{KL} will take on small values. Given that the KL divergence becomes undefined when $q(z|u) = 0$ and $p(z|u) > 0$ for a genre/business z , we instead use:

$$\tilde{q}(z | u) = (1 - \alpha) \cdot q(z | u) + \alpha \cdot p(z | u) \quad (11)$$

By choosing a small and positive α , we ensure that $q \approx \tilde{q}$ while avoiding zero probabilities in q . In our experiments, we set $\alpha = 0.01$ [68].

Popularity Bias. To measure popularity bias, popularity lift PL expresses to what extent the popularity of items in a recommended list of items differs from the popularity of items in a user profile [3, 53], here a positive PL indicates that the algorithm amplifies popularity bias. Popularity lift is computed by comparing the Group Average Popularity $GAP(G)$ items in a user's profile p and items in a recommended list q :

$$PL(G) = \frac{GAP_q(G) - GAP_p(G)}{GAP_p(G)} \quad (12)$$

The $GAP(G)$ takes into account the popularity π_i of all items i in the item lists for all users u in a group G (such as niche or blockbuster) [53]:

$$GAP_p(G) = \frac{\sum_{u \in G} \frac{\sum_{i \in p_u} \pi_i}{|p_u|}}{|G|} \quad (13)$$

Novelty. Novelty evaluates how unexpected the recommended items are to users. If a recommender system heavily relies on a user's past behavior, it may recommend items that are similar to those that the user interacted with before. This can create a feedback loop where users are repeatedly exposed to similar content, reinforcing existing preferences and potentially leading to bias. The concept of novelty refers to having novel elements in the recommended list or the average information surprisal in the recommended item list [70]. Using popularity as a basis for calculating novelty [16, 79, 80], novelty is the average popularity of the N top items:

$$\text{Novelty}(R) = \frac{1}{|R|} \sum_{i \in R} POP_i = \frac{1}{|R|} \sum_{i \in R} -\log(\pi_i) \quad (14)$$

In the equation 14, $|R|$ represents the length of the recommended list, and π_i represents the popularity of item i , i.e., the fraction of users who have rated it positively (for example, ratings greater than a threshold value).

Coverage. Coverage in a recommender system refers to the percentage of items from the total item set I that contained in the list of items R recommended by the system [28]. Formally:

$$\text{Coverage}(I, R) = \frac{|\{i \in I : i \in R\}|}{|I|} \quad (15)$$

Table 3. Average training time and epochs for different models on 1M and Yelp over a set of noise multipliers: (0.2, 0.4, 0.8, 2, 4). These noise multipliers result in different epsilon for different models; the relevant epsilon values do not significantly impact training time per epoch. (Values are averaged, and near-zero standard deviations are not reported)

Privacy	Model	1M		Yelp	
		Time/Epoch (s)	Early Stop Epoch	Time/Epoch (s)	Early Stop Epoch
Non-Private	NCF	70.3 ± 13.2	21 ± 23	27.7 ± 0.0	8.0
	VAE	7.6 ± 0.2	133.0	52.6 ± 6.7	14.0
	SVD	1183.6 ± 754.7	21.3 ± 12.5	5451.3 ± 1359.4	46.0
	BPR	105.9 ± 31.2	48.0	182.0 ± 27.1	43.0
DPSGD for ϵ	NCF	106.8 ± 1.64	18 ± 10	1265.7 ± 33.1	8.0 ± 1.2
	VAE	21.7 ± 0.44	11.0	55.32 ± 6.3	11.0
	SVD	1487.8 ± 702.5	400.0	29559.8 ± 4070.1	400.0
	BPR	91.1 ± 2.7	400.0	24078.1 ± 1944.4	400

To calculate coverage, we consider the entire set of items I that the recommender system could recommend. Coverage evaluates the items that appear in the combined recommendation lists across all users, then calculate the fraction of I represented by these recommended items.

Deviation from Producer Fairness. To evaluate producer or item fairness, we use Deviation from Producer Fairness (DPF) [62]. Intuitively, DPF measures whether popular (short-head) items and unpopular (long-tail) items are getting equal visibility in the recommendation lists. If both groups are shown equally, DPF is close to zero, meaning fair exposure between the two item groups, while positive (negative) DPF means over exposure of popular (unpopular) items.

$$\text{DPF}(I_1, I_2, R) = \text{Coverage}(I_1, R) - \text{Coverage}(I_2, R) \quad (16)$$

3.3.3 Privacy. The privacy budget ϵ quantifies the level of privacy protection provided by a DP mechanism. Privacy budget specifies an upper-bound on our privacy loss. A smaller privacy budget requires the output to be more noisy, often leading to reduced utility. For the LDP mechanism, the value of ϵ is determined before the training process begins, as explained in Section 3.1.1.

For DPSGD, the privacy guarantee at each gradient descent step is characterized by the noise multiplier $\sigma = \frac{\sqrt{2 \log\left(\frac{1.25\delta}{\epsilon}\right)}}{\epsilon}$. This choice of σ ensures that each step satisfies (ϵ, δ) -differential privacy [1]. The total privacy cost across the entire training process is analyzed using a privacy accountant technique. It is important to note that the ϵ values for LDP and DPSGD may not be directly comparable. This means that the same ϵ does not necessarily provide the same level of privacy protection across different mechanisms.

3.4 Implementation and Experimental Settings

We evaluate four recommender algorithms on a range of privacy settings. The RSs are configured by varying the noise multiplier for DPSGD in Opacus, which determines the standard deviation of the Gaussian noise added to the gradients. High noise multipliers lead to smaller privacy budgets ϵ . To calculate the privacy loss of training our models, we adopt PRV approach [30] implemented in Opacus. For LDP, we evaluate the recommendation algorithms by varying the ϵ .

To ensure that all models are evaluated under optimized conditions, we performed hyperparameter tuning for every model, dataset, and privacy mechanism. This tuning acts as an ablation study over the key parameters including batch size, learning rate, clipping bound (gradient norm C), Weight decay and Latent dimensionality. We implement all algorithms in Python/PyTorch. For SVD and BPR, we define user and item embeddings, then train the models using SGD to facilitate the application of DPSGD. For each RS model, we conducted a grid-based ablation study, training multiple configurations and selecting hyperparameters based on utility (NDCG) on the held-out validation set. This approach aligns with common practice in the field, where tuning decisions are typically made based on utility metrics. To ensure reproducibility of our results, our code is available at <https://gitlab.com/dmi-pet-public/parsarad2025privacy>.

For BPR, SVD and NCF, we found that a batch size of 256 and an L2 norm regularization with a weight decay of 10^{-5} provide better utility results. For the VAE model, a higher weight decay of 0.01 shows better utility and stability during training. VAE also used a batch size of 500 for the 1M dataset and 10,000 for the Yelp dataset in the DPSGD state; for both the LDP and non-private settings, a batch size of 5000 was used.

The initial learning rate for BPR and SVD was set to 0.0005 and reduced by a factor of 0.1 if the test loss remained unchanged over four consecutive epochs. For VAE, we used an initial learning rate of 0.001, which similarly reduced it if the test loss stagnated over four consecutive epochs. For NCF, the learning rate was set to 0.0005 for MovieLens and 0.0001 for Yelp. The NCF learning rate was scheduled using a StepLR scheduler, which multiplicatively reduces the learning rate by a factor of 0.9 every four epochs.

The latent dimension For the BPR and SVD algorithms was set to 5 for 1M and 8 for Yelp, based on validation performance. For NCF, the matrix factorization dimension was fixed at 8, and the MLP structure used a 3-layers structure with hidden size of 16, 8, and 4. To prevent overfitting and improve model generalization, we use a dropout rate of 0.5 for NCF.

We train all models for 400 epochs and used early stopping to prevent overfitting: training is stopped if no improvement observed on the validation set for six consecutive epochs. DP noise introduces randomness during training, making single-run results potentially unreliable. Therefore, we executed multiple independent training runs for each model–dataset–privacy configuration to obtain stable and representative averages, to the extent feasible given the substantial training times. Specifically, we perform three runs for BPR/1M and SVD/1M, two runs for BPR/Yelp, SVD/Yelp, and VAE/Yelp, five runs for VAE/1M, and six runs for NCF. Table 3 shows the average training times for each model/dataset combination as well as the early stopping epoch. Note that there was no significant difference in training time depending on ϵ .

4 Results

In this section, we present results for privacy, utility, and bias across four recommender systems on the MovieLens 1M and Yelp datasets. We first show results for the privacy-utility trade-off (Section 4.1), followed by an analysis of privacy-bias trade-offs (Section 4.2) and utility-bias trade-offs (Section 4.3). In each case, we first show overall results for all item and user types combined and then separately analyze popular/unpopular items and blockbuster/diverse/niche users. Finally, we synthesize insights across these dimensions (Section 4.4).

4.1 Privacy-Utility Trade-off

Ranking quality (NDCG). Analyzing the ranking quality in terms of NDCG for different recommender algorithms with privacy protections (Figure 4), we see that ranking quality decreases with lower ϵ , as expected, in almost all cases. Models trained with DPSGD show high sensitivity to ϵ , with a marked decrease in ranking quality for smaller ϵ values.

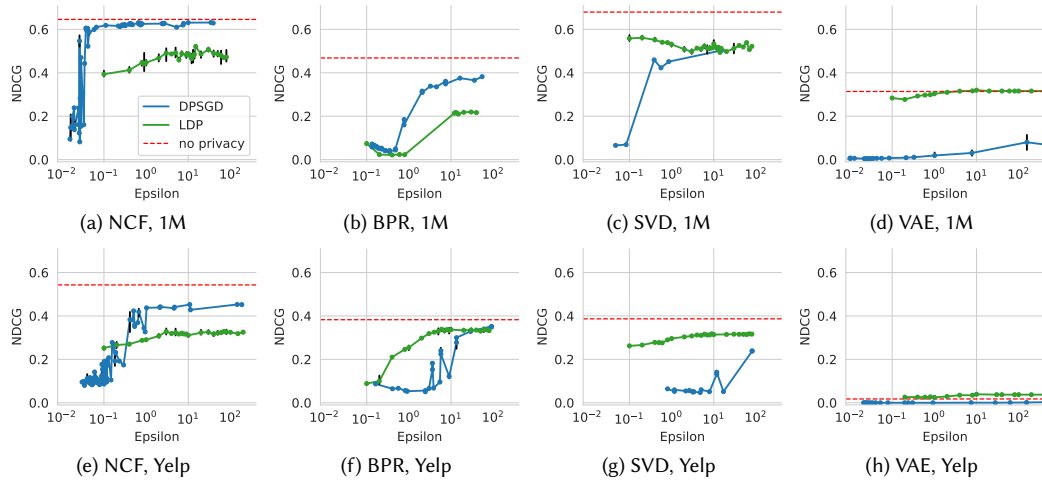


Fig. 4. NDCG Across Different Models and Two Datasets with DPSGD and LDP

In contrast, models trained with LDP show less variation in ranking quality across privacy levels, indicating a more stable but potentially less privacy-sensitive response.

Notably, NCF trained with DPSGD achieves performance comparable to the non-private baseline, even under high privacy constraints ($\epsilon < 1$, see Figures 4a and 4e). This suggests that NCF, when trained with DPSGD, maintains its ranking effectiveness despite differential privacy noise.

LDP outperforms DPSGD in several dataset-model combinations, namely Yelp/SVD (Figure 4g), Yelp/BPR (Figure 4f), 1M/SVD (Figure 4c), and 1M/VAE (Figure 4d). In terms of absolute NDCG, NCF consistently outperforms other models across most datasets and privacy mechanisms. VAE/Yelp, as shown in Figure 4h, has low NDCG in private and non-private settings. Our results show that VAE performs worse on Yelp than on 1M and compared to other algorithms. This weaker performance is consistent with prior studies [6], [40], [12]. A key reason is data sparsity: in our filtered Yelp set, the interaction ratio is only 0.24%, compared to 4.22% for 1M, which weakens the user-item signal².

Differences in evaluation also affect outcomes: prior work often reports NDCG@50 or Recall@100, where VAE performs better, while our stricter NDCG@10 penalizes missing top-ranked items. In addition, Yelp spans a diverse item space (restaurants, shops, services) with strong regional variation, making collaborative filtering harder for generative models like VAE that assume more uniform interaction patterns. Overall, encoding user representations from sparse and diverse data remains a challenge for VAEs [45].

NDCG for Popular vs. Unpopular Items. Analyzing NDCG separately for popular items (I1) and unpopular items (I2) in Figure 5 shows that changes in NDCG with varying ϵ differ between the two item groups. For unpopular items, NDCG is low, and remains largely unaffected by the privacy level (ϵ) under both LDP and DPSGD, suggesting that privacy mechanisms do not significantly alter ranking effectiveness for less frequently recommended items (Figure 5).

²Note that detailed comparisons with prior work are complicated by different preprocessing approaches. Some studies binarize ratings above 4.5 while restricting to restaurants without clear frequency thresholds [6], while others keep the 20 most popular categories and apply 4/10 user-item constraints [12]. Our filtering (ratings ≥ 3 , ≥ 5 reviews per user/item) yields different distributions, and the continuously updated Yelp dataset further increases sparsity compared to the smaller, denser versions used in 2020–2021.

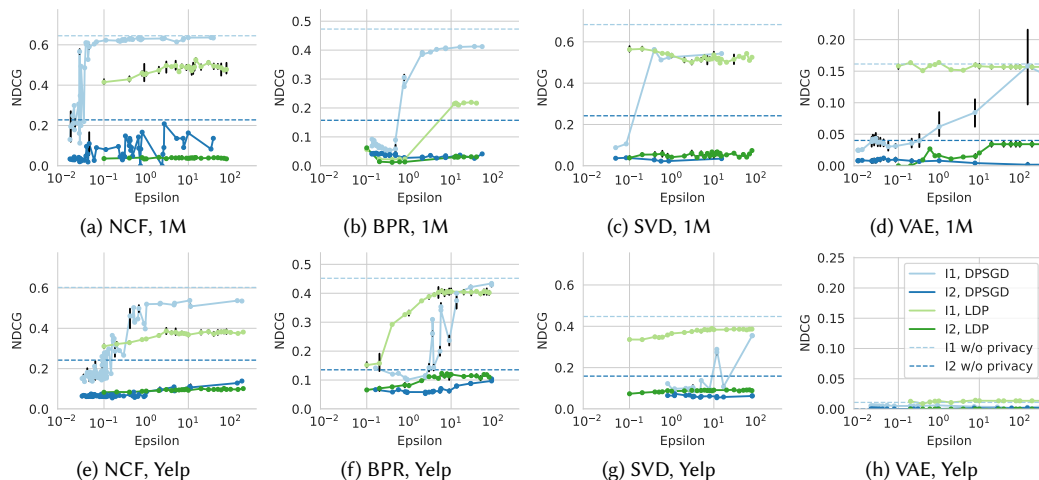


Fig. 5. NDCG for popular items (I1, light colors) and unpopular items (I2, dark colors)

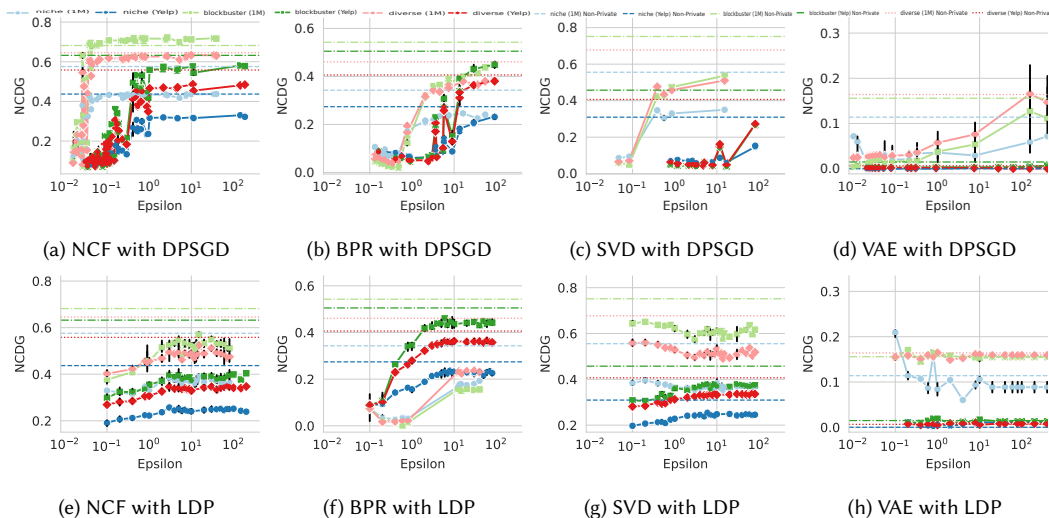


Fig. 6. NDCG by user type (niche (blue circles), diverse (red diamonds), and blockbuster (green squares)) and dataset (Yelp (dark colors) and 1M (light colors))

For popular items, NDCG improves as privacy constraints are relaxed. This means that the improvement in overall NDCG observed in Figure 4 is attributable to an increase in NDCG for popular items, rather than changes in the ranking quality of unpopular items.

NDCG by User Type. Figure 6 presents the NDCG values obtained under LDP and DPSGD across different user types. In most cases, NDCG differs substantially between user groups, indicating that privacy mechanisms affect users with distinct interaction behaviors in different ways. Across all models and datasets, niche users consistently achieve the lowest NDCG values, and their performance plateaus rapidly as ϵ increases. For niche users, NDCG is generally higher

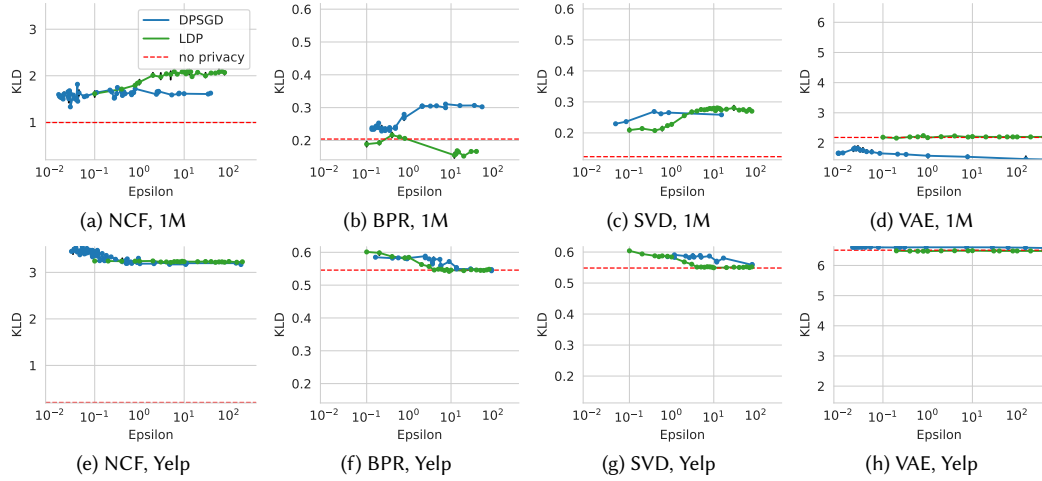


Fig. 7. KLD Across Different Models and Two Datasets with DPSGD and LDP

on 1M than on Yelp (e.g., approximately 0.4 vs. 0.3 for NCF with DPSGD), with one notable exception: for BPR with LDP (Figure 6b), lower ϵ yields slightly higher NDCG on Yelp (0.22 vs. 0.18). For diverse users, NCF (Figures 6a and 6e) achieves the highest NDCG scores, reaching about 0.7 with DPSGD and 0.6 with LDP. In contrast, for blockbuster users, BPR and SVD (Figures 6b–6g) obtain the best performance, typically exceeding 0.4. Finally, VAE (Figures 6d and 6h) performs worst overall, with the most pronounced degradation observed for niche users (NDCG \approx 0).

4.2 Privacy-Bias Trade-off

Miscalibration (KLD). Figure 7 shows the levels of miscalibration, measured by KLD, in our experiments. We can see that whether the use of privacy protections affects miscalibration levels depends on the recommender algorithm. Specifically, miscalibration increases for NCF when privacy mechanisms are applied (Figures 7a and 7e), while miscalibration for other algorithms remains similar to that of the non-private baseline. For all algorithms, there is no significant correlation between the degree of miscalibration and the level of privacy (ϵ).

Popularity Lift. In Figure 8, we report the PL, showing that changes in PL are influenced by both the type of privacy mechanism and the level of privacy applied. Specifically, at high privacy levels, DPSGD tends to produce negative PL values, suggesting that it suppresses recommendations for popular items. While PL generally remains close to the baseline at lower privacy levels, an exception occurs with NCF/DPSGD, which shows a higher PL, as depicted in Figures 8a and 8e. In contrast, LDP shows minimal deviation from the baseline across all models and privacy levels, indicating that it does not introduce substantial bias toward or against popular items. Overall, similar to the baseline, PL for LDP remains consistently positive, indicating that recommendations continue to favor popular items. Popularity lift is generally lower for the Yelp dataset. This may be because the Yelp dataset has a larger item space with sparser interactions. This means that each user interacts with fewer items, and even popular items have fewer total interactions, resulting in less strong signals for the model to confidently overfit to, especially under DP noise.

Novelty. The Novelty results in Figure 9 suggest that privacy constraints may have a dataset-specific influence on novelty. In particular, on the Yelp dataset (bottom row in Figure 9), lower privacy increases novelty, implying that as

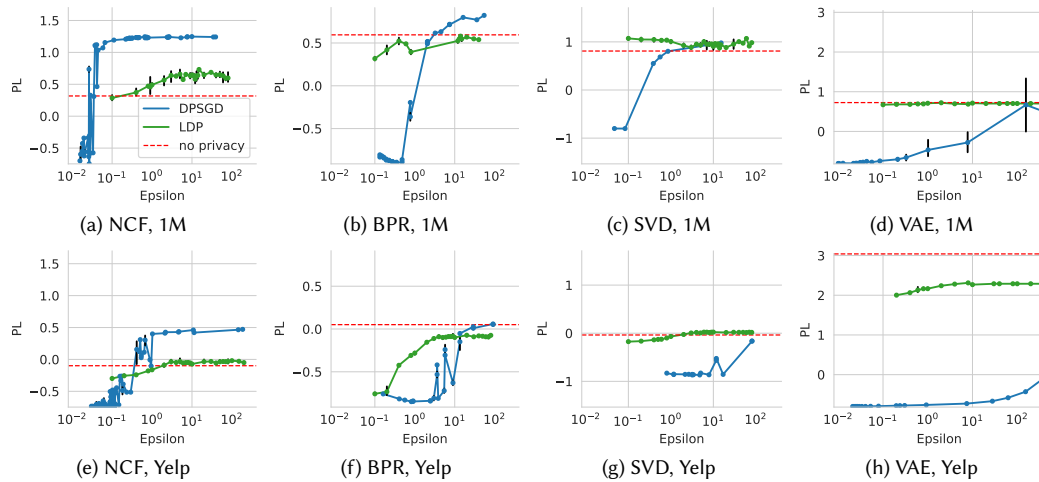


Fig. 8. Popularity Lift Across Different Models and Two Datasets with DPSGD and LDP

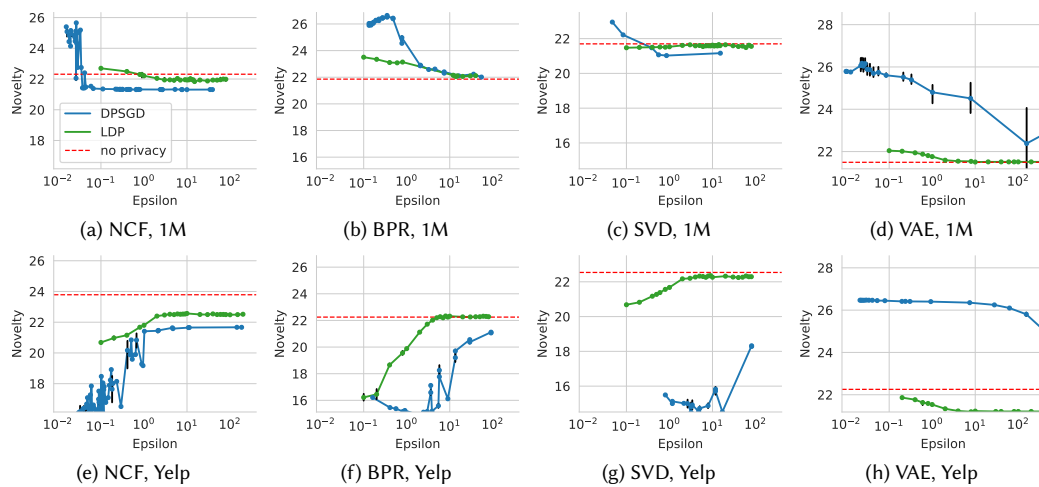


Fig. 9. Novelty Across Different Models and Two Datasets with DPSGD and LDP

privacy constraints are relaxed, the model recommends more diverse and less popular items. Conversely, for the 1M dataset (top row in Figure 9), lower privacy generally decreases novelty.

Coverage. Figure 10 presents the item coverage results, highlighting that the impact of privacy on item coverage is highly model- and dataset-dependent. In particular, NCF/DPSGD (Figures 10a and 10e) significantly reduces coverage, indicating that this combination leads to a concentration of recommendations on a smaller subset of items. In contrast, coverage increases for SVD/DPSGD/1M (Figure 10c), BPR/1M (Figure 10b), and VAE/Yelp (Figure 10h) regardless of privacy levels. For almost all other combinations, coverage remains close to the baseline, suggesting minimal impact.

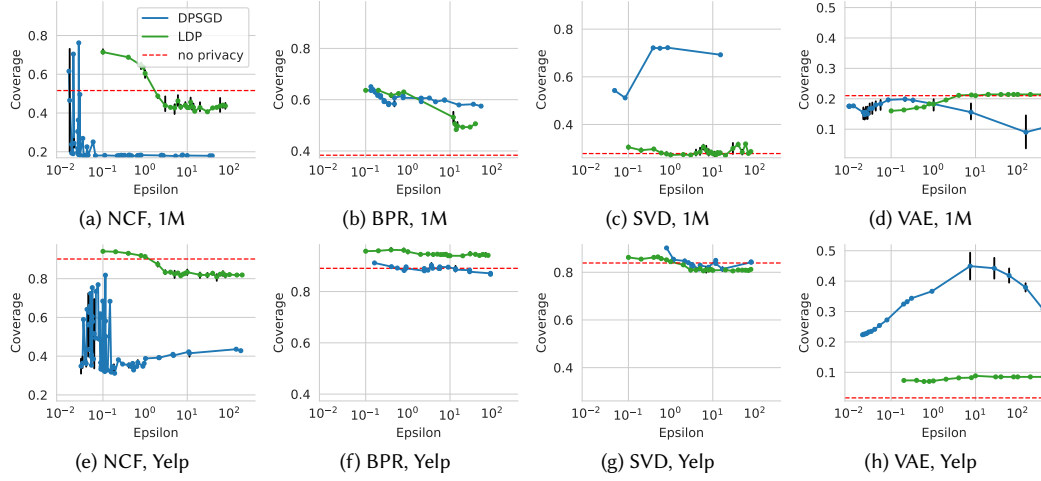


Fig. 10. Coverage Across Different Models and Two Datasets with DPSGD and LDP

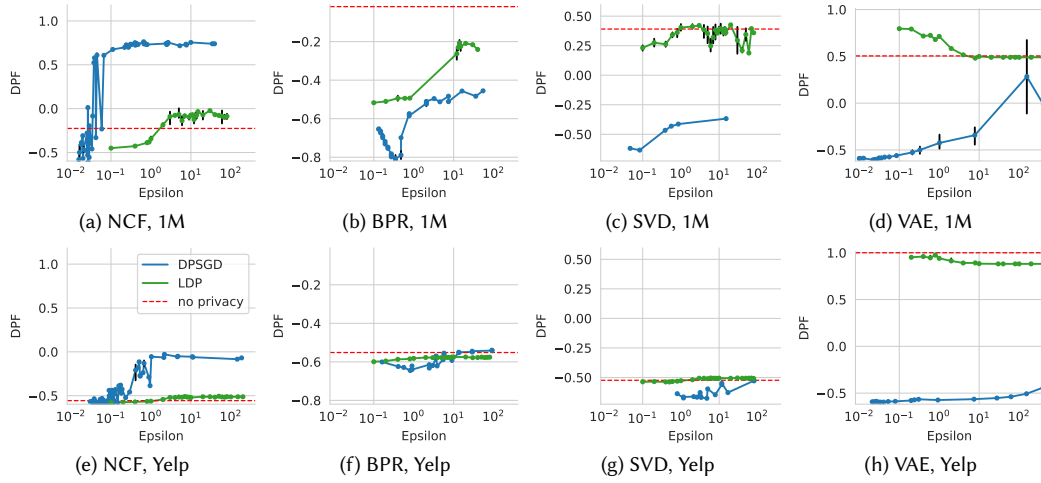


Fig. 11. DPF Across Different Models and Two Datasets with DPSGD and LDP

Deviation from Producer Fairness (DPF). Fairness disparities are measured by DPF (Figure 11) and item exposure. LDP mostly preserves baseline fairness, while DPSGD’s impact varies by dataset. On Yelp, LDP (except VAE/Yelp in Figure 11h) stays close to the baseline, indicating a neutral or mitigating effect on fairness disparity. On 1M, LDP maintains a fairness level of DPF close to the baseline, except for the BPR/1M (Figure 11b) combination, where deviation occurs. Under DPSGD on 1M (e.g., Figures 11b and 11d), DPF decreases and becomes negative under strong privacy constraints, and increases again as the privacy budget grows. In contrast, on Yelp under DPSGD, DPF remains consistently negative across different privacy levels, with minimal variation as ϵ changes. An exception is observed for NCF/Yelp/DPSGD, where DPF increases slightly with larger ϵ , yet it still remains negative (Figure 11e). These results indicate that the impact of privacy-enhancing mechanisms on fairness can differ across datasets.

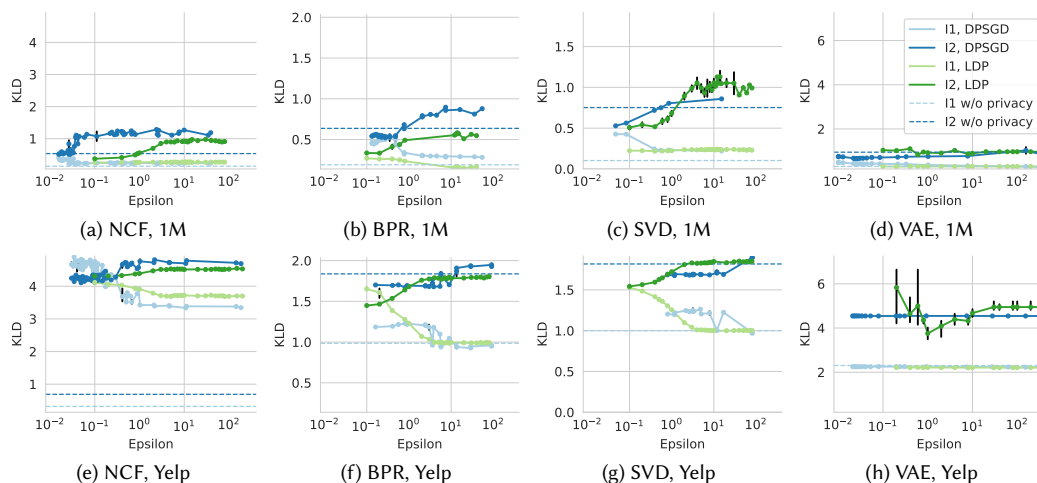


Fig. 12. Miscalibration (KLD) for popular items (I1, light colors) and unpopular items (I2, dark colors)

4.2.1 Privacy-Bias Trade-off by Item Popularity. To further understand the effect of privacy mechanisms, we analyze bias metrics separately for popular and unpopular items.

Miscalibration (KLD) by Item Popularity. Miscalibration, measured by Kullback-Leibler Divergence (KLD) on popular and unpopular items in Figure 12, indicates that popular items are consistently better calibrated than unpopular items, as evidenced by KLD values that are systematically closer to zero (Figure 12). This suggests a smaller divergence between user history and recommendations for popular items. In some algorithm-dataset combinations (eg, BPR/Yelp (Figure 12f) and SVD/Yelp (Figure 12g)), lower privacy levels (higher ϵ) improve calibration for popular items, implying that differential privacy noise can degrade calibration specifically for popular items. Conversely, unpopular items tend to be better calibrated under high privacy levels (smaller ϵ), implying that stronger privacy constraints improve the recommendations for less frequent items.

Popularity Lift (PL) by Item Popularity. Figure 13 shows that the effect of LDP and DPSGD with varying privacy levels (ϵ) on popularity lift (PL) depends on the popularity of items as well as on the recommender algorithm. Across all models and datasets, as ϵ increases, the popularity lift for popular items (I1) grows, indicating that less privacy amplifies popularity bias. Conversely, stronger privacy (smaller ϵ) tends to suppress this bias, reducing the relative advantage of popular items. Overall, differential privacy mechanisms, especially under stricter settings (lower ϵ), can help mitigate popularity bias by preventing models from disproportionately emphasizing popular items.

4.2.2 Privacy-Bias Trade-off by User Type. In this section, we analyze the bias metrics across different user types (niche, blockbuster and diverse), to examine whether bias varies depending on the user type.

Miscalibration (KLD) by User Type. Miscalibration varies across both user groups and datasets (see Figure 14). On Yelp, miscalibration is highest for blockbuster users with BPR (Figures 14b and 14f) and SVD models (Figures 14c and 14g), whereas with NCF (Figures 14a and 14e) and VAE (Figures 14d and 14h) it is highest for niche users. On 1M, miscalibration is highest for niche users across all models and both privacy mechanisms (Figure 14).

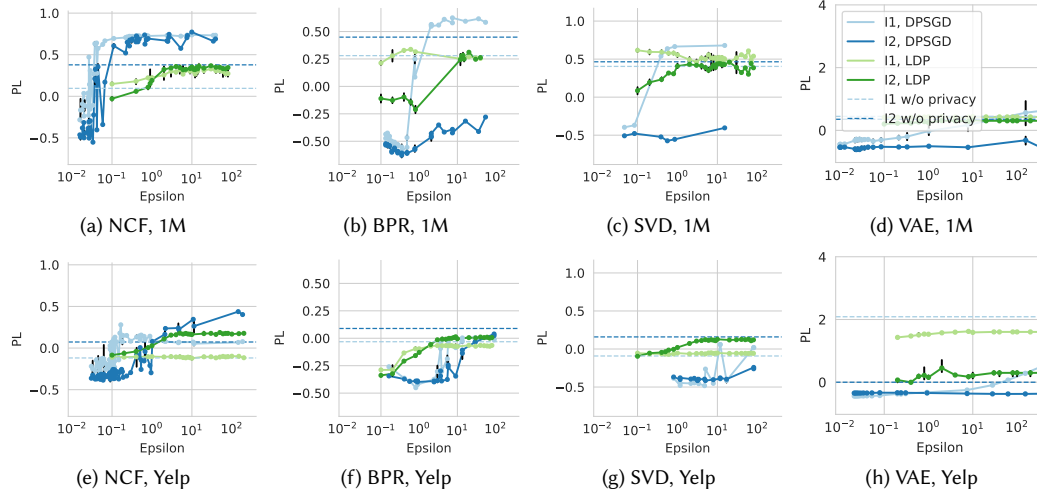


Fig. 13. Popularity lift for popular items (I1, light colors) and unpopular items (I2, dark colors)

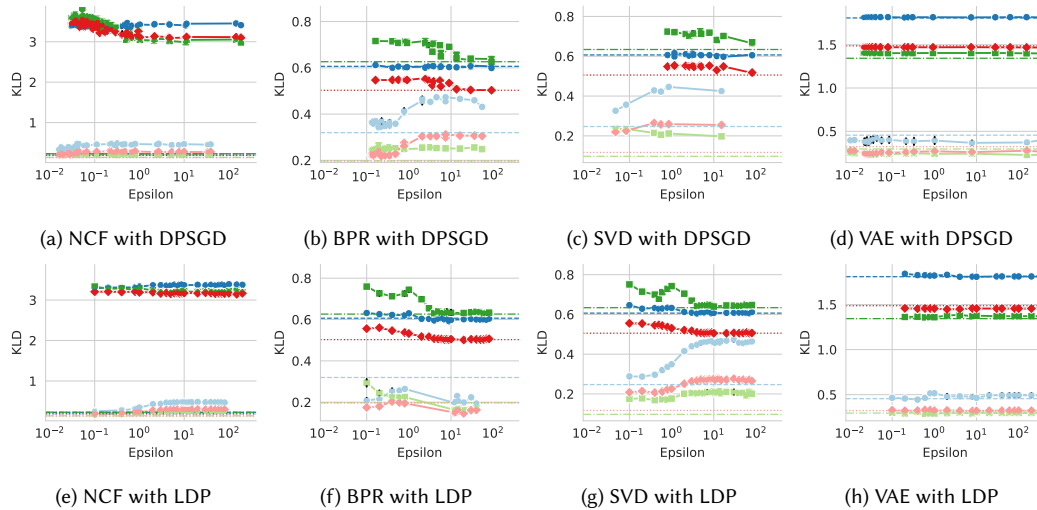


Fig. 14. Miscalibration (KLD) by user group (niche (blue circles), diverse (red diamonds), and blockbuster (green squares)) and dataset (Yelp (dark colors) and 1M (light colors))

Among all model-dataset combinations and user types, NCF on Yelp (Figures 14a and 14e), shows the highest KLD (above 3), whereas all other cases remain below 1, indicating severe miscalibration for this setting. The effect is especially pronounced for niche users. This is likely because NCF achieves high NDCG by heavily favoring popular items, which inherently misaligns with niche users' preferences, resulting in significant distributional mismatch and thus high KLD. On Yelp under LDP, BPR (Figure 14f) and SVD (Figure 14g) have comparable overall KLD and also show the largest KLD disparity across user groups among all models.

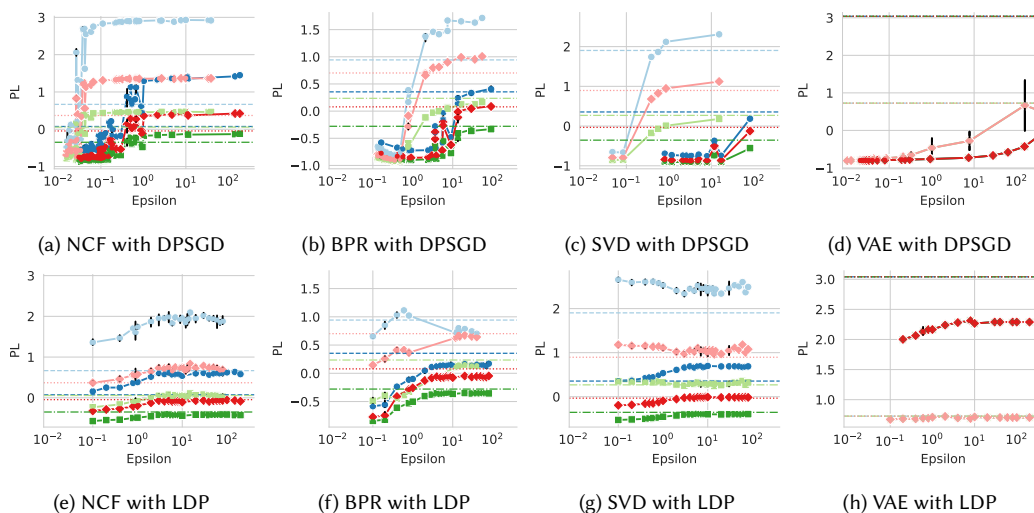


Fig. 15. Popularity lift by user group (niche (blue circles), diverse (red diamonds), and blockbuster (green squares)) and dataset (Yelp (dark colors) and 1M (light colors))

Popularity Lift (PL) by User Type. Figure 15 examines how PL varies for different user types, showing that lower privacy levels generally lead to higher PL across most configurations. Niche users consistently experience the highest popularity lift, suggesting their recommendations are disproportionately skewed toward popular items. An exception occurs for SVD/LDP (Figure 15g), where privacy level does not significantly influence PL. For niche users, the NCF/DPSGD (Figure 15a) and SVD/DPSGD (Figure 15c), PL jumps dramatically at higher epsilon (weaker privacy), reaching values above 2.5. This shows that when privacy constraints are relaxed, the model increasingly pushes popular items to niche users, amplifying the popularity bias. Blockbuster users show moderate PL in most settings, but exceptionally high in VAE/LDP (Figure 15h), suggesting that even popular-item-preferring users receive disproportionately popular recommendations. Diverse users are less affected by popularity amplification, possibly due to their more balanced historical behavior.

Novelty by User Type. Novelty across different user types, as shown in Figure 16, shows that its dependency on ϵ differs between the 1M and Yelp datasets. Intuitively, we expected that novelty would be higher for higher privacy levels because of higher noise levels. This is indeed the case for 1M, however, for Yelp, contrary to expectation, novelty generally increases with lower privacy levels (higher ϵ).

Deviation from Producer Fairness (DPF) by User Type. DPF across different user types (Figure 17) shows that lower privacy generally increases DPF, indicating that higher privacy levels reduce the exposure of popular items. Niche users show the highest DPF in 1M, while diverse users have the highest DPF in Yelp. This indicates that in a 1M dataset, niche users received more popular items than non-popular ones. For all models, datasets, and privacy mechanisms, blockbuster users received more diverse (combination of popular and non-popular items) recommendations; therefore, they have the lowest DPF in different ϵ values.

Coverage I1. In Figure 18, coverage I1 measures the proportion of popular items in recommendation lists (the results for coverage I2, representing the proportion of unpopular items, are not shown because they are exactly reversed). The results show that the user type receiving the highest coverage varies between the Yelp and 1M datasets. Coverage is

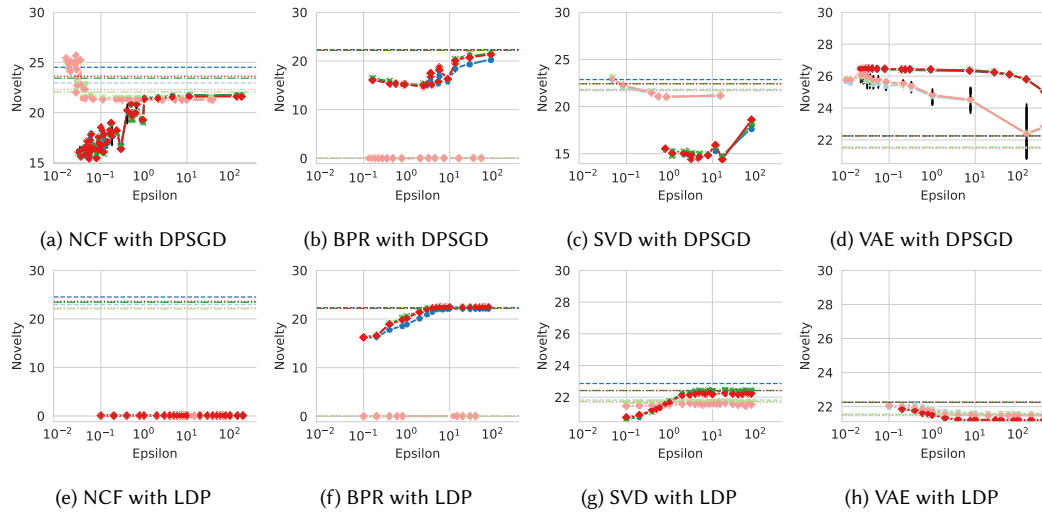


Fig. 16. Novelty by user group (niche (blue circles), blockbuster (red diamonds), and diverse (green squares)) and dataset (Yelp (dark colors) and 1M (light colors))

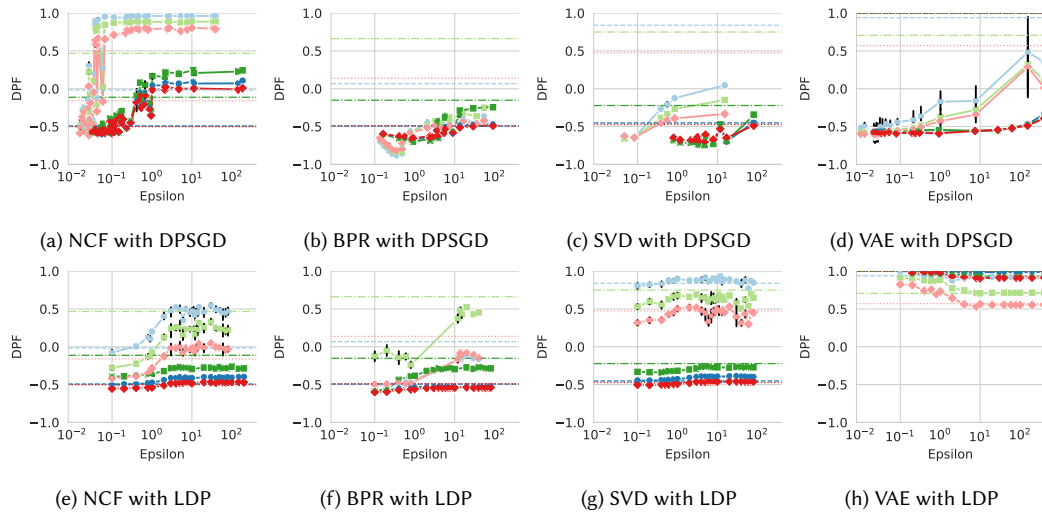


Fig. 17. DPF by user group (niche (blue circles), diverse (red diamonds), and blockbuster (green squares)) and dataset (Yelp (dark colors) and 1M (light colors))

generally highest for niche users, suggesting that they receive a more diverse set of popular items. However, for Yelp, blockbuster users experience the highest coverage of popular items.

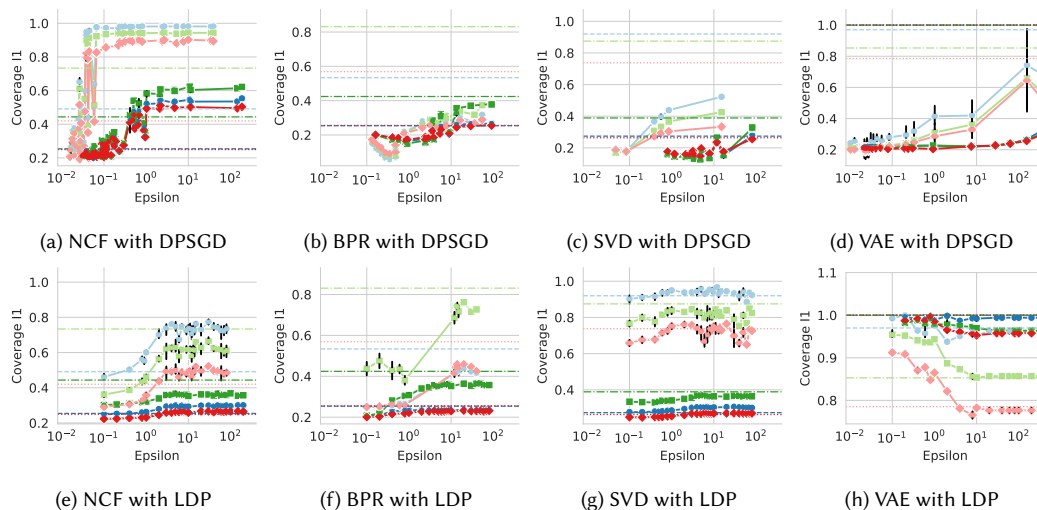


Fig. 18. Coverage I1 by user group (niche (blue circles), diverse (red diamonds), and blockbuster (green squares)) and dataset (Yelp (dark colors) and 1M (light colors))

4.3 Utility-Bias Trade-off

We now discuss the relationships between utility and bias metrics. Figure 19 shows how bias metrics depend on utility levels (measured by ranking quality NDCG), regardless of the privacy level, i.e., Figure 19 includes results for *all* ϵ levels presented in the previous sections.

Miscalibration (KLD). Both LDP and DPSGD show increasing KLD when NDCG rises, meaning that better utility comes at the cost of deviating further from the true user-item interaction distribution. DPSGD tends to produce lower KLD than LDP at similar utility levels, showing slightly better calibration.

Popularity Lift (PL). DPSGD tends to reduce popularity lift (PL of Figure 19) compared to LDP, particularly at lower NDCG values. For both LDP and DPSGD, PL tends to increase toward positive values as NDCG improves, indicating a stronger tendency to recommend popular items when utility increases. Under lower NDCG, DPSGD reduces popularity bias (negative popularity lift) by promoting unpopular items, whereas LDP preserves or exacerbates the baseline popularity bias (positive popularity lift).

Novelty. LDP shows higher novelty when NDCG is higher, as observed for NCF and BPR models. This indicates that LDP can push the recommender to recommend less frequently seen items. DPSGD, however, often sacrifices novelty when NDCG is low.

For 1M, novelty decreases with higher NDCG, whereas for Yelp, it increases. The 1M dataset is relatively dense, with a high overlap across users in the training data (i.e., many users rate the same popular items). Consequently, when the model achieves higher NDCG, it tends to predict mainstream preferences and recommend popular items, resulting in lower novelty. In contrast, the Yelp dataset is much sparser, with highly heterogeneous user interests. As a result, a user’s top recommendations may correspond to less globally popular but personally relevant businesses. Models that effectively learn personalized embeddings can therefore identify less popular yet more relevant items. Hence, in Yelp,

higher NDCG indicates more personalized predictions that deviate from global popularity patterns, leading to higher novelty.

Deviation from Producer Fairness (DPF). Across all models, DPF generally increases with NDCG, indicating that higher-utility (more accurate) models tend to favor popular items, whereas lower-utility models under privacy constraints may give relatively greater exposure to long-tail/unpopular items. Under DPSGD, DPF becomes negative at low NDCG, suggesting that the injected gradient noise reduces the model’s ability to distinguish between frequent and infrequent items. This results in a more uniform exposure distribution, sometimes over-representing unpopular items relative to the head/popular items. However, this apparent fairness improvement is an indirect consequence of degraded model accuracy. In contrast, DPF under LDP remains largely positive, particularly for NCF and BPR, as perturbing individual user ratings preserves existing popularity trends, maintaining a bias toward head items. Overall, DPSGD alters training dynamics more globally, flattening popularity biases while simultaneously lowering recommendation utility.

Summary. These trade-offs suggest DPSGD is preferable for high-utility, fairness-focused systems, while LDP suits applications prioritizing consistent performance.

4.4 Discussion

Our results show nuanced relationships between different DP approaches, their impact on bias metrics, and the trade-offs between privacy, utility, and bias. We now discuss what recommendations can be derived from our experiments for scenarios that require (1) high utility, (2) low bias, and (3) high privacy.

High utility requirement. When maintaining high recommendation accuracy is the primary objective, DPSGD generally outperforms LDP at moderate or relaxed privacy budgets ($\epsilon \geq 1$). Under these settings, DPSGD achieves higher NDCG across models—particularly for NCF—while remaining competitive with the non-private baseline even under $\epsilon < 1$. This advantage arises because DPSGD perturbs gradients during centralized optimization, preserving global patterns across users that are critical for ranking accuracy. In contrast, LDP injects noise locally into each user’s data before aggregation, fragmenting user signals and reducing the model’s ability to generalize collectively.

However, this advantage reverses under strict privacy (very low ϵ), where gradient noise dominates learning dynamics. In such regimes, DPSGD flattens popularity biases but significantly lowers ranking quality. Achieving high utility with DPSGD therefore requires careful tuning of hyperparameters—such as gradient clipping thresholds, learning rates, and batch sizes—to control the trade-off between noise magnitude and convergence. In our experiments, moderate privacy levels ($10^0 < \epsilon < 10^1$) showed the best trade-offs: NCF/DPSGD achieved about 0.6 NDCG on 1M, while BPR/DPSGD reached around 0.4 on both 1M and Yelp.

Although DPSGD is the preferred option for utility-oriented scenarios, its improvements primarily benefit popular items and blockbuster users, leaving long-tail items comparatively underrepresented. Therefore, when maximizing utility under differential privacy, post-processing calibration or re-ranking may be required to maintain recommendation diversity without compromising accuracy.

Low bias requirement. For evaluating popularity bias, We recommended using either PL or DPF, as they follow similar patterns. If the goal is to measure general popularity bias, PL is sufficient, while DPF is preferable when assessing exposure fairness. For fairness evaluation, it is important to consider the coverage of I1 and I2 (rather than looking only at overall item coverage), as this directly reflects exposure imbalance between head/popular and tail/unpopular items.

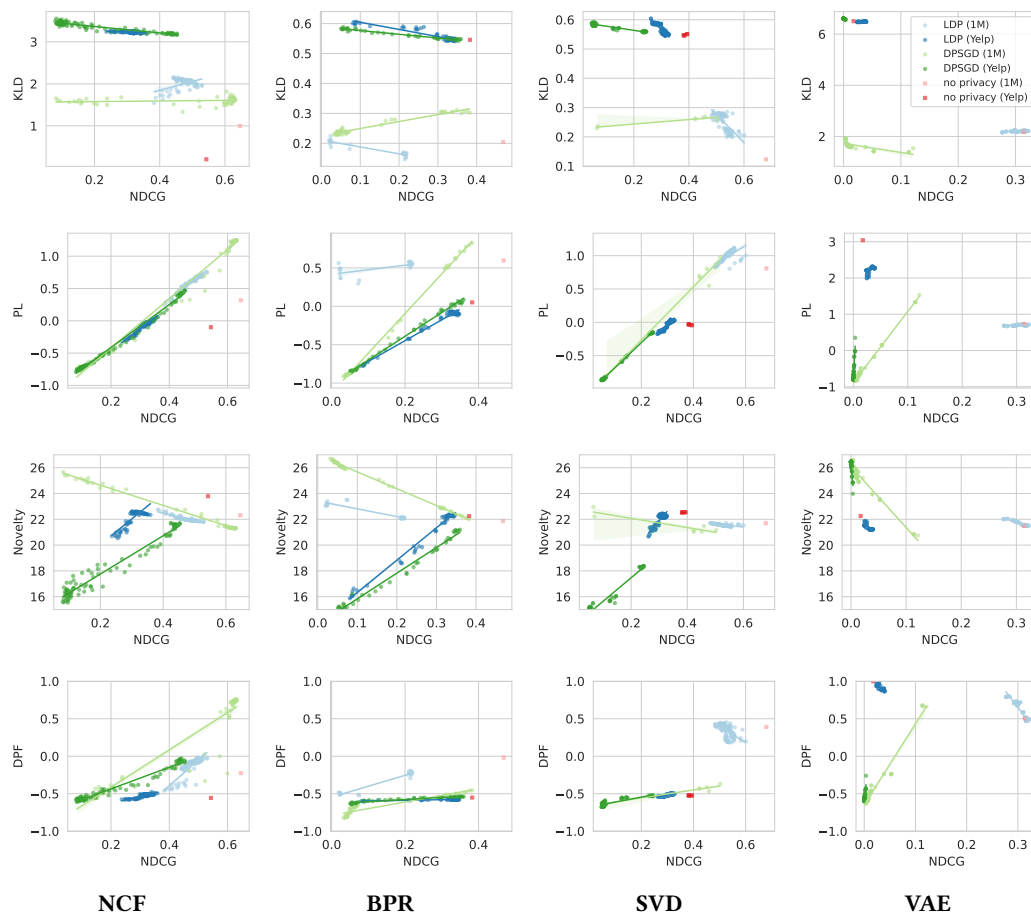


Fig. 19. Utility–bias trade-offs across models evaluated under DPSGD and LDP: The Y-axis shows different bias metrics, the X-axis shows utility (NDCG@10), each row represents a different bias metric, and separate columns correspond to different models. For LDP and DPSGD, each point corresponds to a specific ϵ . The solid line is obtained by fitting a linear regression to the points, showing the trend between utility (NDCG@10) and the corresponding bias metric.

Bias should also be analyzed with respect to user type, since its impact is not uniform across user populations. Niche users typically experience stronger bias toward popular content, especially in denser datasets such as 1M, whereas blockbuster users receive more balanced exposure. Addressing this disproportionate bias requires mechanisms that explicitly mitigate the skew toward popular items.

Existing bias mitigation strategies can be broadly categorized into pre-processing, in-processing, and post-processing approaches. In-processing methods, such as Inverse Propensity Scoring [66] and the Personal Popularity-Aware Counterfactual (PPAC) framework [56], incorporate bias correction into the model’s optimization objective or architecture. However, their impact on DP remains unclear and requires further investigation. Post-processing techniques, on the other hand, modify the recommendations after model training. For example, the Calibrated Popularity [4] greedily minimizes the discrepancy between the distribution of item types in a user’s profile and their recommended list, thereby addressing popularity bias from the users’ perspective. These post-processing approaches benefit from the

post-processing property [21] of the DP mechanism, which ensures that any random, data-independent transformations of differentially private outputs does not compromise privacy guarantees.

Pre-processing approaches also play a role in reducing bias by modifying the dataset before it is fed into the recommender system. For highly sparse datasets (e.g., Yelp), calibration techniques are particularly important to reduce miscalibration, especially for models like NCF trained under privacy constraints. Privacy constraints can exacerbate ranking misalignment, particularly for unpopular items. Calibration ensures that a user’s past interests (for example, their preferred genre distribution) are accurately reflected in their recommended list, maintaining the same proportional representation as in their original preferences [68]. Item feature calibration, such as genre-based calibration, is a post-processing approach and inherently preserves DP. However, implementing calibration requires candidate generation, which can pose privacy risks if not done carefully. Instead of computing scores for all items, recommender systems often rank a smaller candidate set (e.g., the user’s interacted items plus k randomly sampled items). This approach, however, can leak private information if the candidate selection process does not guarantee differential privacy. Therefore, DP-aware candidate generation, such as differentially private sampling, should be employed to ensure privacy, or alternatively, fully random selection may be necessary.

High privacy requirement. Under strict privacy budgets (low ϵ), both LDP and DPSGD cause a clear degradation in ranking quality (NDCG) across models and datasets, with DPSGD showing the strongest sensitivity to privacy strength. For NCF and SVD on 1M, lower ϵ values reduce novelty, implying that privacy noise suppresses exploration of less popular items and reinforces mainstream recommendations. This contrast arises because MovieLens-1M is dense, with high user-item overlap and strong popularity bias, whereas Yelp is sparse and heterogeneous. Thus, in dense datasets, accuracy is driven by popularity alignment (reducing novelty), while in sparse datasets, accuracy stems from personalization (increasing novelty). These opposite trends reflect the role of dataset density: in dense settings, accuracy is driven by popularity alignment, whereas in sparse datasets, accuracy depends on personalized exploration. In practice, we observed reasonable trade-offs for moderate privacy budgets, for instance, NCF on 1M achieves approximately 0.6 NDCG at $\epsilon \approx 10^{-1}$, comparable to higher ϵ values, while NCF/Yelp exceeds 0.4 NDCG at $\epsilon \approx 10^0$; BPR attains about 0.4 NDCG for both datasets within $10^0 < \epsilon < 10^1$.

High privacy also affects fairness and bias differently across datasets. On Yelp, LDP often mitigates fairness disparities (DPF trends toward zero), while on 1M, DPSGD can exacerbate disparities (negative DPF), reflecting a shift toward relatively greater exposure of unpopular items but reduced overall utility. This suggests that dataset characteristics, such as item popularity distribution, influence how privacy mechanisms affect fairness. Popularity lift (PL) further shows that strict privacy (small ϵ) suppresses the amplification of popular items, meaning that both DPSGD and LDP can partially offset inherent popularity bias at the cost of accuracy.

Miscalibration, measured by KLD, remains mostly stable across privacy levels, with one exception: NCF on Yelp shows significantly higher KLD under both DPSGD and LDP. This pattern points to model-specific vulnerabilities in sparse datasets to the privacy-induced noise.

User-group analysis reveals that high privacy intensifies heterogeneity in performance across users. Blockbuster users (those preferring popular items) consistently receive the highest NDCG scores across models and datasets, indicating that privacy mechanisms disproportionately preserve accuracy for users whose behavior aligns with global popularity. In contrast, niche users, who prefer unpopular items, consistently have the lowest NDCG scores, highlighting a utility gap. This disparity implies that strong privacy constraints hinder the model’s ability to recommend relevant long-tail content effectively. Moreover, improvements in overall NDCG as privacy relaxes are primarily driven by popular

items, while unpopular items remain largely unaffected. Similarly, popular items are better calibrated (lower KLD) than unpopular ones, although strict privacy can occasionally narrow this calibration gap by reducing over-confidence in head items.

Overall, high privacy constraints amplify the privacy–utility–fairness tension: while stricter privacy reduces popularity bias and exposure imbalance, it also limits ranking quality, especially for niche users and sparse data regimes. These findings emphasize that achieving equitable and effective recommendations under strong privacy requires model-specific parameter tuning and, potentially, post-processing adjustments for fairness and calibration.

4.5 Sustainability

We estimate energy consumption and carbon emissions for the computations underlying this paper because the global environmental impact of computational activities is an increasingly important concern [41, 58]. Our results were obtained using an NVIDIA GeForce RTX 4090 GPU with a rated power consumption of 450 W [57]. Training our models across four recommender algorithms, ten different noise levels, a non-private baseline, and multiple iterations took approximately 64,000 GPU hours in total (see Appendix A for details). This corresponds to an estimated 28,800 kWh of energy usage³. Using a global average electricity emissions factor of 460 g CO₂/kWh for 2025, this translates to approximately 13.25 metric tons of CO₂ emissions from the training process, nearly equivalent to a full commercial flight’s emissions of 13.8 metric tons [36, 38].

To put that number into perspective, we compare it with the energy consumption of a short-haul flight. An 808km flight from Zurich (ZRH) to London (LHR), typically operated by an Airbus A320, consumes about 52,439 kWh of jet fuel energy, of which around 18,354 kWh are converted to practical work. The GPU training task therefore used approximately 55% of the flight’s total fuel energy, and 157% of its useful energy.

5 Conclusion

In this paper, we presented a comprehensive evaluation of the impact of differentially private training on the performance and bias of recommender systems. Our evaluation considered multiple metrics to measure utility, bias, and privacy, and assessed the effects of both LDP and DPSGD. We experimented with four recommender systems – SVD and BPR as classic approaches, and NCF and VAE as deep learning-based methods – on the MovieLens and Yelp datasets. Our findings highlight how different DP techniques influence various aspects of these models, providing insights into the trade-offs between privacy, accuracy, and bias in recommender systems.

We identified ranges of the privacy budget in which acceptable trade-offs between privacy, accuracy, and bias can be achieved. These findings highlight that practitioners should not rely on a single metric or fixed privacy level; instead, they must systematically experiment with different parameters, such as the choice of ϵ , to determine which configuration best aligns with their priorities. Depending on whether utility, bias mitigation, or calibration is more critical, different parameter settings may produce more desirable outcomes. Consequently, evaluating multiple metrics simultaneously is essential, and the intended objective must be explicitly defined to select the most appropriate privacy configuration.

The results also show several areas that deserve further study, including the effects of the model characteristics on privacy and bias, and the design of more robust models that can better balance privacy and performance. Future work could explore the development of calibration-based post-processing methods that preserve privacy guarantees, as well

³Our estimates exclude energy used by the rest of the system (CPU, cooling, storage, etc.) and do not include time spent on hyperparameter tuning and code debugging, which would further increase energy consumption and emissions.

as extensions to more robust privacy-preserving recommenders. This includes evaluating user-level differential privacy instead of interaction-level protection [24], and integrating embedding-aware noise mechanisms [55] to better preserve representational structure under privacy constraints.

References

- [1] Martin Abadi, Andy Chu, Ian Goodfellow, H. Brendan McMahan, Ilya Mironov, Kunal Talwar, and Li Zhang. 2016. Deep Learning with Differential Privacy. In *Proceedings of the 2016 ACM SIGSAC Conference on Computer and Communications Security*. ACM, Vienna Austria, 308–318. doi:10.1145/2976749.2978318
- [2] Himan Abdollahpour, Masoud Mansoury, Robin Burke, and Bamshad Mobasher. 2019. The Unfairness of Popularity Bias in Recommendation. arXiv:1907.13286 [cs] doi:10.48550/arXiv.1907.13286
- [3] Himan Abdollahpour, Masoud Mansoury, Robin Burke, and Bamshad Mobasher. 2020. The Connection Between Popularity Bias, Calibration, and Fairness in Recommendation. In *Proceedings of the 14th ACM Conference on Recommender Systems (RecSys '20)*. Association for Computing Machinery, Virtual Event Brazil, 726–731. doi:10.1145/3383313.3418487
- [4] Himan Abdollahpour, Masoud Mansoury, Robin Burke, Bamshad Mobasher, and Edward Malthouse. 2021. User-Centered Evaluation of Popularity Bias in Recommender Systems. In *Proceedings of the 29th ACM Conference on User Modeling, Adaptation and Personalization*. ACM, Utrecht Netherlands, 119–129. doi:10.1145/3450613.3456821
- [5] Michael Aerni, Jie Zhang, and Florian Tramèr. 2024. Evaluations of Machine Learning Privacy Defenses Are Misleading. arXiv:2404.17399 [cs] doi:10.1145/3658644.3690194
- [6] Diego Antognini and Boi Faltings. 2021. Fast Multi-Step Critiquing for VAE-based Recommender Systems. In *Fifteenth ACM Conference on Recommender Systems*. ACM, Amsterdam Netherlands, 209–219. doi:10.1145/3460231.3474249
- [7] Aviex Flight School. n.d.. *How Much Fuel Do Commercial Planes Use?* <https://aviex.goflexair.com/flight-school-training-faq/how-much-fuel-do-commercial-planes-use> Accessed: 2025-05-06.
- [8] Eugene Bagdasaryan, Omid Poursaeed, and Vitaly Shmatikov. 2019. Differential Privacy Has Disparate Impact on Model Accuracy. In *Proceedings of the 33rd International Conference on Neural Information Processing Systems*. Number 1387. Curran Associates Inc., Red Hook, NY, USA, 15479–15488.
- [9] Christine Bauer, Eva Zangerle, and Alan Said. 2024. Exploring the Landscape of Recommender Systems Evaluation: Practices and Perspectives. *ACM Trans. Recomm. Syst.* 2, 1 (March 2024), 11:1–11:31. doi:10.1145/3629170
- [10] Bin Bi, Milad Shokouhi, Michal Kosinski, and Thore Graepel. 2013. Inferring the Demographics of Search Users: Social Data Meets Search Queries. In *Proceedings of the 22nd International Conference on World Wide Web*. ACM, Rio de Janeiro Brazil, 131–140. doi:10.1145/2488388.2488401
- [11] Franziska Boenisch, Adam Dziedzic, Roei Schuster, Ali Shahin Shamsabadi, Ilia Shumailov, and Nicolas Papernot. 2023. When the Curious Abandon Honesty: Federated Learning Is Not Private. In *2023 IEEE 8th European Symposium on Security and Privacy (EuroS&P)*. IEEE Computer Society, 175–199. doi:10.1109/EuroSP57164.2023.00020
- [12] Tommaso Carraro, Mirko Polato, and Fabio Aioli. 2020. Conditioned Variational Autoencoder for Top-N Item Recommendation. arXiv:2004.11141 [cs] doi:10.48550/arXiv.2004.11141
- [13] Jiawei Chen, Hande Dong, Xiang Wang, Fuli Feng, Meng Wang, and Xiangnan He. 2023. Bias and Debias in Recommender System: A Survey and Future Directions. *ACM Transactions on Information Systems* 41, 3 (July 2023), 1–39. doi:10.1145/3564284
- [14] Zhili Chen, Yu Wang, Shun Zhang, Hong Zhong, and Lin Chen. 2021. Differentially Private User-Based Collaborative Filtering Recommendation Based on k-Means Clustering. *Expert Systems with Applications* 168 (April 2021), 114366. doi:10.1016/j.eswa.2020.114366
- [15] Mihaela Curmei, Walid Krichene, Li Zhang, and Mukund Sundararajan. 2023. Private Matrix Factorization with Public Item Features. In *Proceedings of the 17th ACM Conference on Recommender Systems*. ACM, Singapore, 805–812. doi:10.1145/3604915.3608833
- [16] Diego Corrêa da Silva, Marcelo Garcia Manzato, and Frederico Araújo Durão. 2021. Exploiting Personalized Calibration and Metrics for Fairness Recommendation. *Expert Systems with Applications* 181 (Nov. 2021), 115112. doi:10.1016/j.eswa.2021.115112
- [17] Yashar Deldjoo. 2024. Understanding Biases in ChatGPT-based Recommender Systems: Provider Fairness, Temporal Stability, and Recency. *ACM Trans. Recomm. Syst.* (Aug. 2024). doi:10.1145/3690655
- [18] Yashar Deldjoo, Dietmar Jannach, Alejandro Bellogin, Alessandro Difonzo, and Dario Zanzonelli. 2024. Fairness in Recommender Systems: Research Landscape and Future Directions. *User Modeling and User-Adapted Interaction* 34, 1 (March 2024), 59–108. doi:10.1007/s11257-023-09364-z
- [19] Angela Di Fazio. 2024. Enhancing Privacy in Recommender Systems through Differential Privacy Techniques. In *Proceedings of the 18th ACM Conference on Recommender Systems (RecSys '24)*. Association for Computing Machinery, New York, NY, USA, 1348–1352. doi:10.1145/3640457.3688019
- [20] Bolin Ding, Janardhan Kulkarni, and Sergey Yekhanin. 2017. Collecting Telemetry Data Privately. In *Proceedings of the 31st International Conference on Neural Information Processing Systems (NIPS'17)*. Curran Associates Inc., Red Hook, NY, USA, 3574–3583.
- [21] Cynthia Dwork and Aaron Roth. 2014. The Algorithmic Foundations of Differential Privacy. *Foundations and Trend in Theoretical Computer Science* 9, 3–4 (Aug. 2014), 211–407. doi:10.1561/04000000042
- [22] Mehdi Elahi, Danial Khosh Kholgh, Mohammad Sina Kiarostami, Soroush Saghari, Shiva Parsa Rad, and Marko Tkalčič. 2021. Investigating the Impact of Recommender Systems on User-Based and Item-Based Popularity Bias. *Information Processing & Management* 58, 5 (Sept. 2021), 102655. doi:10.1016/j.ipm.2021.102655

- [23] Odai Enaizan, A. A. Zaidan, N. H. M. Alwi, B. B. Zaidan, M. A. Alsalem, O. S. Albahri, and A. S. Albahri. 2020. Electronic Medical Record Systems: Decision Support Examination Framework for Individual, Security and Privacy Concerns Using Multi-Perspective Analysis. *Health and Technology* 10, 3 (May 2020), 795–822. doi:10.1007/s12553-018-0278-7
- [24] Le Fang, Bingqian Du, and Chuan Wu. 2022. Differentially Private Recommender System with Variational Autoencoders. *Knowledge-Based Systems* 250 (Aug. 2022), 109044. doi:10.1016/j.knosys.2022.109044
- [25] Le Fang, Bingqian Du, and Chuan Wu. 2022. Differentially Private Recommender System with Variational Autoencoders. *Knowledge-Based Systems* 250 (Aug. 2022), 109044. doi:10.1016/j.knosys.2022.109044
- [26] Leonardo Ferreira, Daniel Castro Silva, and Mikel Uriarte Itzazelaia. 2023. Recommender Systems in Cybersecurity. *Knowledge and Information Systems* 65, 12 (Dec. 2023), 5523–5559. doi:10.1007/s10115-023-01906-6
- [27] Christian Ganhör, David Penz, Navid Rekasaz, Oleg Lesota, and Markus Schedl. 2022. Unlearning Protected User Attributes in Recommendations with Adversarial Training. In *Proceedings of the 45th International ACM SIGIR Conference on Research and Development in Information Retrieval*. ACM, Madrid Spain, 2142–2147. doi:10.1145/3477495.3531820
- [28] Mouzhi Ge, Carla Delgado-Battenfeld, and Dietmar Jannach. 2010. Beyond Accuracy: Evaluating Recommender Systems by Coverage and Serendipity. In *Proceedings of the Fourth ACM Conference on Recommender Systems*. ACM, Barcelona Spain, 257–260. doi:10.1145/1864708.1864761
- [29] Yingqiang Ge, Shuchang Liu, Zuohui Fu, Juntao Tan, Zelong Li, Shuyuan Xu, Yunqi Li, Yikun Xian, and Yongfeng Zhang. 2024. A Survey on Trustworthy Recommender Systems. *ACM Trans. Recomm. Syst.* (April 2024). doi:10.1145/3652891
- [30] Sivakanth Gopi, Yin Tat Lee, and Lukas Wutschitz. 2021. Numerical Composition of Differential Privacy. In *Advances in Neural Information Processing Systems*, Vol. 34. Curran Associates, Inc., 11631–11642.
- [31] David M. Greenberg, Michal Kosinski, David J. Stillwell, Brian L. Monteiro, Daniel J. Levitin, and Peter J. Rentfrow. 2016. The Song Is You: Preferences for Musical Attribute Dimensions Reflect Personality. *Social Psychological and Personality Science* 7, 6 (Aug. 2016), 597–605. doi:10.1177/1948550616641473
- [32] Aniko Hannak, Piotr Sapiezynski, Arash Molavi Kakhki, Balachander Krishnamurthy, David Lazer, Alan Mislove, and Christo Wilson. 2013. Measuring Personalization of Web Search. In *Proceedings of the 22nd International Conference on World Wide Web (WWW '13)*. ACM, Rio de Janeiro, Brazil, 527–538. doi:10.1145/2488388.2488435
- [33] F. Maxwell Harper and Joseph A. Konstan. 2016. The MovieLens Datasets: History and Context. *ACM Transactions on Interactive Intelligent Systems* 5, 4 (Jan. 2016), 1–19. doi:10.1145/2827872
- [34] Xiangnan He, Lizi Liao, Hanwang Zhang, Liqiang Nie, Xia Hu, and Tat-Seng Chua. 2017. Neural Collaborative Filtering. In *Proceedings of the 26th International Conference on World Wide Web (WWW '17)*. International World Wide Web Conferences Steering Committee, Geneva, Switzerland, 173–182. doi:10.1145/3038912.3052569
- [35] Yassine Himeur, Shahab Saquib Sohail, Faycal Bensaali, Abbes Amira, and Mamoun Alazab. 2022. Latest Trends of Security and Privacy in Recommender Systems: A Comprehensive Review and Future Perspectives. *Computers & Security* 118 (July 2022), 102746. doi:10.1016/j.cose.2022.102746
- [36] International Civil Aviation Organization. 2020. Freighter Methodology Version 2.0. https://applications.icao.int/icec/Freighter_Methodology_v2.0_Final.pdf Accessed May 9, 2025.
- [37] International Energy Agency. 2019. *Global Energy & CO2 Status Report 2019*. Technical Report. International Energy Agency, Paris. <https://www.iea.org/reports/global-energy-co2-status-report-2019> Accessed: 2025-05-09.
- [38] International Energy Agency. 2025. *Electricity 2025*. Technical Report. International Energy Agency, Paris. <https://www.iea.org/reports/electricity-2025> Accessed: 2025-05-09.
- [39] Aryan Jadon and Avinash Patil. 2025. A Comprehensive Survey of Evaluation Techniques for Recommendation Systems. In *Computation of Artificial Intelligence and Machine Learning*, Amit Kumar Bairwa, Varun Tiwari, Santosh Kumar Vishwakarma, Milan Tuba, and Thittaporn Ganokratanaa (Eds.). Springer Nature Switzerland, Cham, 281–304. doi:10.1007/978-3-031-71484-9_25
- [40] Giannis Karamanolakis, Kevin Raji Cherian, Ananth Ravi Narayan, Jie Yuan, Da Tang, and Tony Jebara. 2018. Item Recommendation with Variational Autoencoders and Heterogeneous Priors. In *Proceedings of the 3rd Workshop on Deep Learning for Recommender Systems*. ACM, Vancouver BC Canada, 10–14. doi:10.1145/3270323.3270329
- [41] Loïc Lannelongue, Jason Grealey, and Michael Inouye. 2021. Green Algorithms: Quantifying the Carbon Footprint of Computation. *Advanced Science* 8, 12 (2021), 2100707. doi:10.1002/advs.202100707
- [42] Jure Leskovec, Daniel Huttenlocher, and Jon Kleinberg. 2010. *On the Efficiency of Social Recommender Networks*. Technical Report. Yelp Dataset Challenge. https://www.yelp.com/html/pdf/YelpDatasetChallengeWinner_NetworkEfficiency.pdf
- [43] Xueqi Li, Guoqing Xiao, Yuedan Chen, Zhuo Tang, Wenjun Jiang, and Kenli Li. 2023. An Explicitly Weighted GCN Aggregator Based on Temporal and Popularity Features for Recommendation. *ACM Trans. Recomm. Syst.* 1, 2 (April 2023), 8:1–8:23. doi:10.1145/3587272
- [44] Dawen Liang, Rahul G. Krishnan, Matthew D. Hoffman, and Tony Jebara. 2018. Variational Autoencoders for Collaborative Filtering. arXiv:1802.05814 [cs, stat]
- [45] Shangsong Liang, Zhou Pan, wei liu, Jian Yin, and Maarten de Rijke. 2024. A Survey on Variational Autoencoders in Recommender Systems. *Comput. Surveys* 56, 10 (Oct. 2024), 1–40. doi:10.1145/3663364
- [46] Dugang Liu, Pengxiang Cheng, Hong Zhu, Zhenhua Dong, Xiuqiang He, Weike Pan, and Zhong Ming. 2023. Debaised Representation Learning in Recommendation via Information Bottleneck. *ACM Trans. Recomm. Syst.* 1, 1 (Jan. 2023), 5:1–5:27. doi:10.1145/3568030

- [47] Ziqi Liu, Yu-Xiang Wang, and Alexander Smola. 2015. Fast Differentially Private Matrix Factorization. In *Proceedings of the 9th ACM Conference on Recommender Systems*. ACM, Vienna Austria, 171–178. doi:10.1145/2792838.2800191
- [48] Daniele Malatesta, Giandomenico Cornacchia, Claudio Pomo, Felice Antonio Merra, Tommaso Di Noia, and Eugenio Di Sciascio. 2024. Formalizing Multimedia Recommendation through Multimodal Deep Learning. *ACM Trans. Recomm. Syst.* (April 2024). doi:10.1145/3662738
- [49] Rachana Mehta and Keyur Rana. 2017. A Review on Matrix Factorization Techniques in Recommender Systems. In *2017 2nd International Conference on Communication Systems, Computing and IT Applications (CSCITA)*. 269–274. doi:10.1109/CSCITA.2017.8066567
- [50] Jacob M Miracle. 2016. *De-Anonymization Attack Anatomy and Analysis of Ohio Nursing Workforce Data Anonymization*. Ph. D. Dissertation. Wright state University, Dayton, Ohio.
- [51] Peter Müllner, Elisabeth Lex, Markus Schedl, and Dominik Kowald. 2023. Differential Privacy in Collaborative Filtering Recommender Systems: A Review. *Frontiers in Big Data* 6 (Oct. 2023), 1249997. doi:10.3389/fdata.2023.1249997
- [52] Peter Müllner, Elisabeth Lex, Markus Schedl, and Dominik Kowald. 2024. The Impact of Differential Privacy on Recommendation Accuracy and Popularity Bias. In *Advances in Information Retrieval*, Nazli Goharian, Nicola Tonello, Yulan He, Aldo Lipani, Graham McDonald, Craig Macdonald, and Iadh Ounis (Eds.). Springer Nature Switzerland, Cham, 466–482. doi:10.1007/978-3-031-56066-8_33
- [53] Mohammadmehdi Naghiaei, Hossein A. Rahmani, and Mahdi Dehghan. 2022. The Unfairness of Popularity Bias in Book Recommendation. In *Advances in Bias and Fairness in Information Retrieval*, Ludovico Boratto, Stefano Faralli, Mirko Marras, and Giovanni Stilo (Eds.). Springer International Publishing, Cham, 69–81. doi:10.1007/978-3-031-09316-6_7
- [54] Tien T. Nguyen, Pik-Mai Hui, F. Maxwell Harper, Loren Terveen, and Joseph A. Konstan. 2014. Exploring the Filter Bubble: The Effect of Using Recommender Systems on Content Diversity. In *Proceedings of the 23rd International Conference on World Wide Web (WWW '14)*. Association for Computing Machinery, New York, NY, USA, 677–686. doi:10.1145/2566486.2568012
- [55] Lin Ning, Steve Chien, Shuang Song, Mei Chen, Yunqi Xue, and Devora Berlowitz. 2022. EANA: Reducing Privacy Risk on Large-scale Recommendation Models. In *Proceedings of the 16th ACM Conference on Recommender Systems*. ACM, Seattle WA USA, 399–407. doi:10.1145/3523227.3546769
- [56] Wentao Ning, Reynold Cheng, Xiao Yan, Ben Kao, Nan Huo, Nur Al Hasan Haldar, and Bo Tang. 2024. Debiasing Recommendation with Personal Popularity. In *Proceedings of the ACM Web Conference 2024*. ACM, Singapore Singapore, 3400–3409. doi:10.1145/3589334.3645421
- [57] NVIDIA. n.d. *GeForce RTX 4090*. <https://www.nvidia.com/de-de/geforce/graphics-cards/40-series/rtx-4090/> Accessed: 2025-05-06.
- [58] David Patterson, Joseph Gonzalez, Quoc Le, Chen Liang, Lluís-Miquel Munguia, Daniel Rothchild, David So, Maud Texier, and Jeff Dean. 2021. Carbon Emissions and Large Neural Network Training. arXiv:2104.10350 [cs] doi:10.48550/arXiv.2104.10350
- [59] Kuei-Hsiang Peng, Li-Heng Liou, Cheng-Shang Chang, and Duan-Shin Lee. 2015. Predicting Personality Traits of Chinese Users Based on Facebook Wall Posts. In *2015 24th Wireless and Optical Communication Conference (WOCC)*. IEEE, Taipei, Taiwan, 9–14. doi:10.1109/WOCC.2015.7346106
- [60] Dana Pessach and Erez Shmueli. 2022. A Review on Fairness in Machine Learning. *ACM Comput. Surv.* 55, 3 (Feb. 2022), 51:1–51:44. doi:10.1145/3494672
- [61] Nikolaos Polatidis, Christos K. Georgiadis, Elias Pimenidis, and Emmanouil Stiakakis. 2017. Privacy-Preserving Recommendations in Context-Aware Mobile Environments. *Information & Computer Security* 25, 1 (March 2017), 62–79. doi:10.1108/ICS-04-2016-0028
- [62] Hossein A. Rahmani, Mohammadmehdi Naghiaei, and Yashar Deldjoo. 2024. A Personalized Framework for Consumer and Producer Group Fairness Optimization in Recommender Systems. *ACM Trans. Recomm. Syst.* 2, 3 (June 2024), 19:1–19:24. doi:10.1145/3651167
- [63] Rouzbeh Razavi. 2020. Personality Segmentation of Users through Mining Their Mobile Usage Patterns. *International Journal of Human-Computer Studies* 143 (Nov. 2020), 102470. doi:10.1016/j.ijhcs.2020.102470
- [64] Steffen Rendle, Christoph Freudenthaler, Zeno Gantner, and Lars Schmidt-Thieme. 2009. BPR: Bayesian Personalized Ranking from Implicit Feedback. In *Proceedings of the Twenty-Fifth Conference on Uncertainty in Artificial Intelligence (UAI '09)*. AUAI Press, Arlington, Virginia, USA, 452–461.
- [65] Steffen Rendle and Li Zhang. 2023. On Reducing User Interaction Data for Personalization. *ACM Trans. Recomm. Syst.* 1, 3 (Aug. 2023), 14:1–14:28. doi:10.1145/3600097
- [66] Tobias Schnabel, Adith Swaminathan, Ashudeep Singh, Navin Chandak, and Thorsten Joachims. 2016. Recommendations as Treatments: Debiasing Learning and Evaluation. arXiv:1602.05352 [cs] doi:10.48550/arXiv.1602.05352
- [67] Sulthana Shams and Douglas Leith. 2024. Evaluating Impact of User-Cluster Targeted Attacks in Matrix Factorisation Recommenders. *ACM Trans. Recomm. Syst.* (June 2024). doi:10.1145/3674157
- [68] Harald Steck. 2018. Calibrated Recommendations. In *Proceedings of the 12th ACM Conference on Recommender Systems*. ACM, Vancouver British Columbia Canada, 154–162. doi:10.1145/3240323.3240372
- [69] Kiran Tomlinson, Mengting Wan, Cao Lu, Brent Hecht, Jaime Teevan, and Longqi Yang. 2023. Targeted Training for Multi-organization Recommendation. *ACM Transactions on Recommender Systems* 1, 3 (Sept. 2023), 1–18. doi:10.1145/3603508
- [70] Isabel Wagner and David Eckhoff. 2018. Technical Privacy Metrics: A Systematic Survey. *ACM Comput. Surv.* 51, 3 (June 2018), 57:1–57:38. doi:10.1145/3168389
- [71] Xiangmeng Wang, Qian Li, Dianer Yu, Qing Li, and Guandong Xu. 2024. Constrained Off-policy Learning over Heterogeneous Information for Fairness-aware Recommendation. *ACM Trans. Recomm. Syst.* 2, 4 (July 2024), 29:1–29:27. doi:10.1145/3629172
- [72] Udi Weinsberg, Smriti Bhagat, Stratis Ioannidis, and Nina Taft. 2012. BlurMe: Inferring and Obfuscating User Gender Based on Ratings. In *Proceedings of the Sixth ACM Conference on Recommender Systems*. ACM, Dublin Ireland, 195–202. doi:10.1145/2365952.2365989
- [73] Emre Yalcin and Alper Bilge. 2021. Investigating and Counteracting Popularity Bias in Group Recommendations. *Information Processing & Management* 58, 5 (Sept. 2021), 102608. doi:10.1016/j.ipm.2021.102608

- [74] Fajie Yuan, Xiangnan He, Alexandros Karatzoglou, and Liguang Zhang. 2020. Parameter-Efficient Transfer from Sequential Behaviors for User Modeling and Recommendation. In *Proceedings of the 43rd International ACM SIGIR Conference on Research and Development in Information Retrieval (SIGIR '20)*. Association for Computing Machinery, New York, NY, USA, 1469–1478. doi:10.1145/3397271.3401156
- [75] Eva Zangerle and Christine Bauer. 2022. Evaluating Recommender Systems: Survey and Framework. *ACM Comput. Surv.* 55, 8 (Dec. 2022), 170:1–170:38. doi:10.1145/3556536
- [76] Richard Zemel, Yu Wu, Kevin Swersky, Toniann Pitassi, and Cynthia Dwork. 2013. Learning Fair Representations. In *Proceedings of the 30th International Conference on International Conference on Machine Learning - Volume 28 (ICML '13)*. JMLR.org, Atlanta, GA, USA, III–325–III–333.
- [77] Shuai Zhang, Lina Yao, Aixin Sun, and Yi Tay. 2020. Deep Learning Based Recommender System: A Survey and New Perspectives. *Comput. Surveys* 52, 1 (Jan. 2020), 1–38. doi:10.1145/3285029
- [78] Yang Zhang, Zhiyu Hu, Yimeng Bai, Jiancan Wu, Qifan Wang, and Fuli Feng. 2024. Recommendation Unlearning via Influence Function. *ACM Trans. Recomm. Syst.* (Oct. 2024). doi:10.1145/3701763
- [79] Yuan Cao Zhang, Diarmuid Ó Séaghdha, Daniele Quercia, and Tamas Jambor. 2012. Auralist: Introducing Serendipity into Music Recommendation. In *Proceedings of the Fifth ACM International Conference on Web Search and Data Mining*. ACM, Seattle Washington USA, 13–22. doi:10.1145/2124295.2124300
- [80] Tao Zhou, Zoltán Kuscik, Jian-Guo Liu, Matúš Medo, Joseph Rushton Wakeling, and Yi-Cheng Zhang. 2010. Solving the Apparent Diversity–Accuracy Dilemma of Recommender Systems. *Proceedings of the National Academy of Sciences* 107, 10 (March 2010), 4511–4515. doi:10.1073/pnas.1000488107

Appendix

A Sustainability Calculations

In this section, we report the average energy consumption required to produce the results presented in this paper, focusing on the GPU training tasks. Our approach estimates the total energy consumed by the NVIDIA GeForce RTX 4090 graphics card during model training, expressed in kilowatt-hours (kWh). To provide context and make these numbers more tangible, we compare this energy consumption to that of a typical short-haul flight on an Airbus A320, calculating both the energy content of the fuel burned and the resulting carbon dioxide (CO_2) emissions in metric tons. Finally, we estimate the carbon emissions attributable to the GPU training and compare these to the flight emissions, highlighting the environmental impact of computational workloads.

For our training task, completing one epoch across the four approaches, 10 different noise/epsilon levels, and one non-private case requires approximately 160 hours. With an average of 100 epochs per noise/epsilon level, the total training time per noise/epsilon level (in a single replication) is:

$$160 \text{ hours/run} \times 100 \text{ runs} = 16,000 \text{ hours}$$

The results are based on different iterations per setting (as explained in Section 3.4), here we consider in average 4 iterations which leading to a total training time of:

$$\frac{16,000 \text{ hours}}{\text{iteration}} \times 4 \text{ iterations} = 64,000 \text{ hours}$$

Therefore, the total energy consumed by the RTX 4090 for making this table is: $64,000 \text{ hours} \times 0.45 \text{ kW} = 28,800 \text{ kWh}$. The flight distance between Zurich (ZRH) and London (LHR) is approximately 808 km, typically covered by a short-haul aircraft like the Airbus A320 in 1.75 hours. Airbus A320 consumes approximately 2,500 kg of Jet A-1 fuel per hour during flight [7]. For a 1.75-hour flight, the total fuel consumption is: $2,500 \text{ kg/hour} \times 1.75 \text{ hours} = 4,375 \text{ kg}$. Jet A-1 fuel has an energy content of 43.15 MJ/kg (43,150,000 J/kg). The total energy content of the fuel is: $4,375 \text{ kg} \times 43,150,000 \text{ J/kg} = 188,781,250,000 \text{ J}$. Converting to kilowatt-hours (1 kWh = 3,600,000 J): $\frac{188,781,250,000 \text{ J}}{3,600,000} = 52,439 \text{ kWh}$. Jet engines have an efficiency of approximately 30–40% in converting fuel energy to practical work (e.g., thrust). Assuming 35% efficiency, the useful energy output is: $52,439 \text{ kWh} \times 0.35 = 18,354 \text{ kWh}$. The RTX 4090's training task consumes 28,800 kWh,

which is approximately 55% of the flight's total fuel energy (52,439 kWh), and is approximately 157% of the flight's useful energy output (18,354 kWh).

For Jet A-1 fuel, the emission factor is approximately 3.16 ([36]). This emission factor is the number of tonnes of CO₂ produced by burning a tonne of aviation fuel. Based on the consumed fuel and the emission factor, the total emission is: $4,375 \text{ kg fuel} \times 3.16 \frac{\text{kg CO}_2}{\text{kg fuel}} = 13,825 \text{ kg CO}_2$. This is approximately 13.8 metric tons of CO₂ for one flight. The RTX 4090 training task's carbon emissions are calculated using a global average emission factor for electricity of 460 g CO₂/kWh for 2025. This value is estimated by applying a 3% reduction in emissions intensity, as reported for 2024 [38], to the 2018 baseline of 475 g CO₂/kWh [37]. For 28,800 kWh, the emissions are:

$$28,800 \text{ kWh} \times 0.46 \frac{\text{kg CO}_2}{\text{kWh}} = 13,248 \text{ kg CO}_2 \approx 13.25 \text{ metric tons CO}_2. \quad (17)$$

This emission level is more than a full flight's emissions.